


ORIGINAL ARTICLE

Spinal Nrf2 translocation may inhibit neuronal NF- κ B activation and alleviate allodynia in a rat model of bone cancer pain

Jie Fu | Chaobo Ni | Hua-Dong Ni | Long-Sheng Xu | Qiu-Li He | Huan Pan | Dong-Dong Huang | Yan-Bao Sun | Ge Luo | Ming-Juan Liu | Ming Yao 

Department of Anesthesiology and Pain Research Center, The First Hospital of Jiaying or The Affiliated Hospital of Jiaying University, Jiaying, China

Correspondence

Ming Yao, Department of Anesthesiology and Pain Research Center, The First Hospital of Jiaying or The Affiliated Hospital of Jiaying University, Jiaying, 314001, China.
Email: jxyaoming666@163.com.

Funding information

National Natural Science Foundation of China, Grant/Award Number: 81901124 and 82001176; Natural Science Foundation of Zhejiang Province of China, Grant/Award Number: LY20H090020, LGF20H090021 and LQ19H090007; Medical and Health Science and Technology Research Program of Zhejiang Province, Grant/Award Number: 2020RC124 and 2020RC122; Science and Technology Project of Jiaying City, Grant/Award Number: 2020AY30009; Key Discipline Established by Zhejiang Province and Jiaying City Jointly -Pain Medicine, Grant/Award Number: 2019-ss-ttyx; Key Discipline of Anesthesiology of Jiaying City and Jiaying Key Laboratory of Neurology and Pain Medicine, Grant/Award Number: 2019-zc-06

Abstract

Bone cancer pain (BCP) is a clinical pathology that urgently needs to be solved, but research on the mechanism of BCP has so far achieved limited success. Nuclear factor erythroid 2 (NFE2)-related factor 2 (Nrf2) has been shown to be involved in pain, but its involvement in BCP and the specific mechanism have yet to be examined. This study aimed to test the hypothesis that BCP induces the transfer of Nrf2 from the cytoplasm to the nucleus and further promotes nuclear transcription to activate heme oxygenase-1 (HO-1) and inhibit the activation of nuclear factor-kappa B (NF- κ B) signalling, ultimately regulating the neuroinflammatory response. Von-Frey was used for behavioural analysis in rats with BCP, whereas western blotting, real-time quantitative PCR (RT-PCR) and enzyme-linked immunosorbent assay (ELISA) were used to detect molecular expression changes, and immunofluorescence was used to detect cellular localization. We demonstrated that BCP induced increased Nrf2 nuclear protein expression with decreased cytoplasmic protein expression in the spinal cord. Further increases in Nrf2 nuclear protein expression can alleviate hyperalgesia and activate HO-1 to inhibit the expression of NF- κ B nuclear protein and inflammatory factors. Strikingly, intrathecal administration of the corresponding siRNA reversed the above effects. In addition, the results of double immune labelling revealed that Nrf2 and NF- κ B were coexpressed in spinal cord neurons of rats with BCP. In summary, these findings suggest that the entry of Nrf2 into the nucleus promotes the expression of HO-1, inhibiting activation of the NF- κ B signalling pathway, reducing neuroinflammation and ultimately exerting an anti-nociceptive effect.

Abbreviations: 3D, three-dimensional; ANOVA, analysis of variance; AP-1, activator protein 1; ARE, anti-oxidant response element; BCA, biconchonic acid; BCP, bone cancer pain; CFA, complete freund's adjuvant; CT, computed tomography; CX3CL1, C-X3-C motif chemokine 1; CXCL1, chemokine (C-X-C motif) ligand 1; DMSO, dimethyl sulphoxide; ELISA, enzyme-linked immunosorbent assay; GFAP, glial fibrillary acidic protein; HDAC3, histone deacetylase 3; HO-1, heme oxygenase-1; IBA-1, ionized calcium binding adapter molecule 1; IL-6, interleukin-6; IL- β , interleukin-1beta; iNOS, inducible nitric oxide synthase; KEAP1, kelch-like ECH-related protein 1; LPS, lipopolysaccharide; MAPK, mitogen-activated protein kinase; NeuN, neuronal nuclei; NF- κ B, Nuclear factor-kappa B; Nrf2, Nuclear factor erythroid 2 (NFE2)-related factor 2; PBS, phosphate-buffered saline; PWT, paw withdrawal threshold; ROS, reactive oxygen species; RT-PCR, real-time quantitative PCR; SD, sprague-dawley; SFN, sulforaphane; siRNA, small interfering RNA; STR, short tandem repeat; TNF- α , tumour necrosis factor alpha.

This is an open access article under the terms of the Creative Commons Attribution-NonCommercial-NoDerivs License, which permits use and distribution in any medium, provided the original work is properly cited, the use is non-commercial and no modifications or adaptations are made.

© 2021 The Authors. *Journal of Neurochemistry* published by John Wiley & Sons Ltd on behalf of International Society for Neurochemistry

KEYWORDS

bone cancer pain, HO-1, neuroinflammation, NF- κ B, Nrf2, nuclear translocation

1 | INTRODUCTION

Bone cancer pain (BCP) is a chronic pain and a severe complication of malignancy that is characterized by hyperalgesia and allodynia (Buga & Sarria, 2012; Wang et al., 2020). Previous studies have shown that BCP occurs in approximately 21% of the cancer patients who die of cancer, which severely affects the quality of life in these patients and increases the social burden (Kane et al., 2015; Turabi & Plunkett, 2012). Although several recent studies have made significant progress in exploring the pathophysiology of BCP, the specific cellular and molecular mechanisms remain elusive (Mantyh, 2014; von Moos et al., 2017).

Oxidative stress is associated with many diseases, including heart disease, respiratory diseases, neurodegenerative diseases, gastrointestinal diseases and cancer (Pauwels et al., 2007; Young & Woodside, 2001). Accumulating evidence shows that oxidative stress triggers and maintains pain by activating glutamate signaling pathways and inflammatory pathways, as well as by directly affecting nociceptive centres in the brain (Nashed et al., 2014). In BCP models, oxidative stress alters the response of primary afferent neurons to glutamate by inducing cancer cells to produce glutamate as an allogenic and nitrifying substance that participates in the progression and maintenance of cancer-induced chronic pain (Lozano-Ondoua et al., 2013).

Nuclear factor erythroid 2 (NFE2)-related factor 2 (Nrf2) is a member of the cap 'n' collar (CNC) subfamily of basic region leucine zipper (bZip) transcription factors (Ma, 2013). Under normal physiological conditions, Kelch-like ECH-related protein 1 (Keap1) binds to Nrf2 in the cytoplasm (Cho et al., 2006; Villeneuve et al., 2010), which inhibits the transcriptional activity of Nrf2 via ubiquitination and proteasomal degradation (Wang et al., 2014). Under oxidative stress, Nrf2 dissociates from its interaction with Keap1 because of the thiol modification of Keap1 cysteine residues, which ultimately prevents Nrf2 ubiquitination and proteasomal degradation (Hayes et al., 2010). Subsequently, Nrf2 translocates into the nucleus, heterodimerizes with small Maf proteins and binds with the anti-oxidant response element (ARE) to mediate the transcription of several anti-oxidant genes, including heme oxygenase-1 (HO-1) (Suzuki et al., 2013; Tebay et al., 2015), ultimately inhibiting the expression of a variety of inflammatory molecules, such as tumour necrosis factor- α (TNF- α), interleukin-1 β (IL- β) and interleukin-6 (IL-6) (Kensler et al., 2013; Zhang & Hannink, 2003). Previous studies indicated that Nrf2 and HO-1 may be involved in pain. Intraperitoneal administration of sulforaphane (SFN), an activator of the transcription factor Nrf2, reduces inflammatory pain (Redondo et al., 2017) and neuropathic pain (Ferreira-Chamorro et al., 2018) by activating Nrf2 to inhibit glial cell activation and the release of inflammatory factors. In addition, intraperitoneal administration of HO-1 receptor

agonists significantly promoted the expression of opioid receptors in the spinal cord of neuropathic pain model rats (Hervera et al., 2013) and inhibited rodent inflammatory visceral pain (Devesa et al., 2005; Hervera et al., 2013), as well as neuropathic pain related to type 1 diabetes (Hervera et al., 2012). However, the specific mechanism of Nrf2 in BCP models remains unclear.

Nuclear factor-kappa B (NF- κ B) is a widely studied transcription factor. Some studies have shown that NF- κ B mediates C-X3-C motif chemokine 1 (CX3CL1), chemokine (C-X-C motif) ligand 1 (CXCL1) and other chemokines to cause chronic pain after tissue injury or nerve injury (Berti-Mattera et al., 2011; Xu et al., 2014; Yin et al., 2015). Previous studies have also confirmed that NF- κ B participates in pain by regulating the release of inflammatory factors, such as inducible nitric oxide synthase (iNOS) (Wang et al., 2018). Several examples demonstrated that there is direct or indirect activation and inhibition between the Nrf2 and NF- κ B pathways (Ahmed et al., 2017). In response to lipopolysaccharide (LPS) stimulation, Nrf2 knockdown significantly increased NF- κ B transcriptional activity and NF- κ B-dependent gene transcription, indicating that Nrf2 inhibits NF- κ B transcriptional activity (Hwang et al., 2013; Thimmulappa et al., 2006). However, this mechanism has not been confirmed in the BCP rat model.

In this study, we hypothesized that promoting the transfer of Nrf2 from the cytoplasm to the nucleus inhibits NF- κ B from entering the nucleus by activating HO-1, which alleviates allodynia in rats with BCP by reducing the neuroinflammatory response (release of inflammatory factors) in the spinal cord. To test this hypothesis, we studied the expression and subcellular localization of Nrf2 and NF- κ B in the dorsal horn of the spinal cord of the BCP rat model. In addition, we also used corresponding drug interventions to observe the expression of corresponding molecules and behavioural changes in rats with BCP. Finally, the expression of inflammatory factors was also determined.

2 | MATERIALS AND METHODS

2.1 | Experimental animals

A total of 355 female Sprague-Dawley (SD) rats (RRID:RGD_10395233, aged 6 weeks, 160–180 g) were purchased from Shanghai Leagene Biotech Co., Ltd (NO.202000062). At the beginning of the experiment, SD rats were randomly assigned to six rats per cage. Rat cage size was 545 × 395 × 200 mm. All rats were kept in a breeding room at constant temperature (22 ± 2°C), and adequate food and water were supplied. The rats were adapted to the experimental environment for 2 days before the experiment. The researchers optimized the content of the experiment,



chose the best experimental scheme and reduced the number of animals as much as possible. Referring to the previous literature (Fulas et al., 2020; Hu et al., 2017; Ma et al., 2020), sodium pentobarbital was used to anaesthetize rats. Sodium pentobarbital was finally configured to a final concentration of 5 mg/ml solution to avoid irritation. All animal experiments were performed between 8:00 and 20:00. During the operation, a heating blanket was used to keep the body temperature stable, and all operators skilfully mastered the related surgery for the experiment to shorten the operation time. After surgery, wounds were topically disinfected with 75% (v/v) ethanol, but not systemic antibiotics to avoid interference with experimental pharmacological treatments. Because the purpose of the current study was to examine a chronic pain state, no analgesics were used during behavioural assessment to prevent distortion of the results. At the end of the experiment, rats were killed with excessive anaesthetics while not in the presence of other rats. All efforts were made to minimize the suffering of animals. All experimental procedures were approved by the Animal Use and Care Committee for Research and Education of the Jiaxing University (Jiaxing, China) and conducted in accordance with the ethical guidelines to investigate experimental pain in conscious animals (Zimmermann, 1986). Ethics approval reference number: JUMC2020-018.

2.2 | Experimental design

The study described in this manuscript was not pre-registered and was exploratory. The timeline of each experiment along with the number of rats used in each experiment is shown in Figure 1. A total of 355 female SD rats were used in this experiment. Although no statistical method was used to determine the sample number in advance, we determined the required sample size for each group with reference to the previous literature in this field. The behavioural experiments were 6 rats per group (Ni et al., 2019), 4 rats per group for western blot (He et al., 2020) and immunofluorescence (Ni et al., 2020), 5 rats per group for real-time quantitative PCR (Mohamed et al., 2020) and enzyme-linked immunosorbent assay (Zhang et al., 2019) and 10 rats per group for computed tomography (CT) reconstruction and histological analysis of bone (Xu et al., 2019). Referring to the previous literature (Ma et al., 2020), the animals were simply randomly grouped. For example, in the Figure 1a, 52 rats were artificially numbered 1–52, and then each rat corresponded to a pseudorandom number generated by computer software on the order of 1–52. Subsequently, 52 rats were renumbered 1–52 in the order of the pseudorandom numbers from smallest to largest. Finally, the top 26 rats were divided into the sham group, and the rest were divided into the BCP group. In other experiments, rats were grouped in this way as well. In the behavioural experiment, the treated animals were evaluated before the control animals. The preparation of the model and the administration of drugs in animals were performed by one person, and the behavioural tests were performed by another person to achieve blinding of the experimental

groups. Subsequent molecular experiments were performed by researchers who were not involved in the previous two operations. Data analysis was not blinded (Ma et al., 2020).

The weight of all rats was evaluated before the start of the experiment, and those weighing less than 160 g or more than 180 g were removed. All rats met the health standards and were tested for basic pain thresholds. Rats that did not meet the baseline criteria were excluded. In this experiment, no animals died and no animals were replaced or excluded. No adverse drug reactions were observed and animals were constantly monitored throughout the experiment. All data points are reserved, and the specific exclusion criteria are shown in the following experimental methods.

2.3 | Preparation of tumour cells

Rat breast carcinoma cell line, Walker 256 (RRID:CVCL_4984), was used to establish the BCP model. The primary cells were a kind gift from Nanjing University of Chinese Medicine. Based on the previous cancer cell preparation process (Mao-Ying et al., 2006; Yao et al., 2011), Walker 256 cells were injected intraperitoneally into female SD rats. After 1 week, ascites was collected, and cancer cells were extracted.

2.4 | Bone cancer pain model

According to previous studies (Usui et al., 2016; Wang et al., 2011, 2021), rats were anaesthetized by intraperitoneal injection of 50 mg/kg sodium pentobarbital. After making a shallow incision, the lower 1/3 of the left tibia of the rat was exposed, and a hole was drilled. Then, a total of 10 μ l of suspension containing 5×10^5 cancer cells or heat-killed cells was injected into the bone cavity. The syringe was kept stationary to prevent cell leakage and removed after 1 min. The injection site was sealed with bone wax after the syringe was removed. Then, the wound was closed after careful disinfection with 75% (v/v) ethanol.

2.5 | Intrathecal catheterization

Based on previous studies (He et al., 2018; Niu et al., 2017; Tang et al., 2012), a PE-10 microtube (Kang Mei Biological Co) was inserted into the intervertebral space between L4 and L5 for drug delivery. Rats were anaesthetized by intraperitoneal injection of sodium pentobarbital (50 mg/kg), their back hair was shaved. The superficial musculature of the lower back of the rat was sutured after disinfection with 75% (v/v) ethanol, and the catheter was tunnelled subcutaneously to exit through a small incision at the back of the neck (Guo et al., 2017). To confirm that the catheter was located in the subarachnoid space after the operation, 10 μ l lidocaine (2%) was injected through the catheter. Only those rats that showed complete

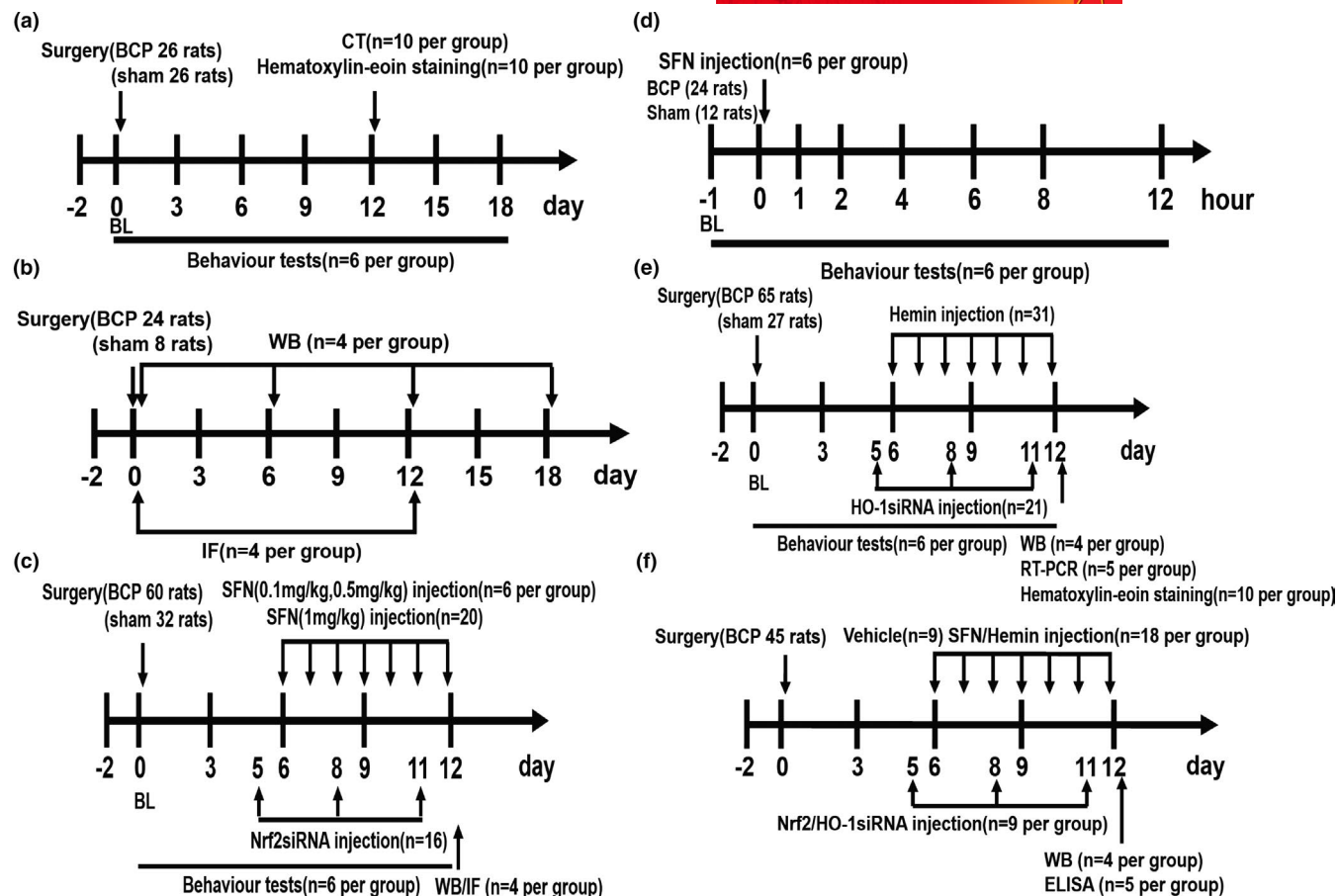


FIGURE 1 The following flow chart includes all the study designs. A total of 355 rats were used in this experiment. Figure 1a corresponds to the experimental steps in Figure 2. To verify whether the bone cancer pain (BCP) model was successfully established, the baseline pain threshold was determined before the operation, and the behaviour test was performed 3, 6, 9, 12, 15 and 18 days after the operation. CT scanning and haematoxylin–eosin staining were performed on the 12th day after the operation in the sham group and BCP groups. Figure 1b corresponds to the experimental steps in Figures 3, 4, 7 and 8a. The dynamic expression of nuclear factor erythroid 2 (NFE2)-related factor 2 (Nrf2), heme oxygenase-1 (HO-1) and nuclear factor-kappa B (NF- κ B) in the spinal cord was detected by western blot (WB) analysis at 0, 6, 12 and 18 days after tumour inoculation. The spinal cords of sham and BCP12 rats were collected for immunofluorescence (IF) to detect the cellular localization of Nrf2, HO-1 and NF- κ B. Figure 1c corresponding to Figure 5a, c–f, and illustrates effects of intrathecal injection of sulforaphane (SFN) and Nrf2 siRNA on mechanical hyperalgesia in rats with BCP. The spinal cord of sham and BCP12 rats was collected for WB and IF to detect molecular expression and cell localization. Figure 1d corresponds to the experimental steps in Figure 5b. Single-dose SFN was administered intrathecally to rats on day 12 after surgery in this experiment. The paw withdrawal threshold (PWT) was measured 1, 2, 4, 6, 8 and 12 hr after drug administration. Figure 1e HO-1 is involved in the regulation of BCP. The experimental steps correspond to results shown in Figure 6a–e, g. Effects of hemin or HO-1 siRNA treatment on mechanical hyperalgesia in rats with BCP. Rats were killed after 12 days of BCP to collect spinal cord and tibia tissues for WB, real-time quantitative PCR and haematoxylin–eosin staining. Figure 1f corresponds to Figure 8b–g. The rats in the model group received the corresponding drug intervention from days to 6–12 after the operation. The spinal cord was collected 12 days after the operation to determine the expression of NF- κ B nuclear protein and related inflammatory factors. BL, baseline. ELISA, enzyme-linked immunosorbent assay. The number of experimental animals was indicated in parenthesis

paralysis of both hind limbs after lidocaine administration were used in subsequent experiments.

2.6 | Drugs

SFN (Nrf2 agonist, purity 99.75%, Cat. No:HY-13755) and hemin (HO-1 agonist, purity: >98.0%, Cat. No:HY-19424) were purchased from MedChemExpress. SFN was solubilized in 3% DMSO

(Cat. No:D2650, Sigma–Aldrich), and hemin was sequentially dissolved in 10% DMSO (Cat. No:D2650, Sigma–Aldrich), 40% PEG300 (Cat. No:HY-Y0873, MedChemExpress), 5% Tween-80 (Cat. No:HY-Y1891, MedChemExpress) and 45% saline sequentially. SFN (0.1, 0.5 and 1 mg/kg, 20 μ l) was administered via an intrathecal catheter. Hemin was selected for intraperitoneal injection (10 mg/kg, 2 ml) to observe changes in pain behaviour. These drugs were administered once a day for 1 week starting on day 6 after the surgery.

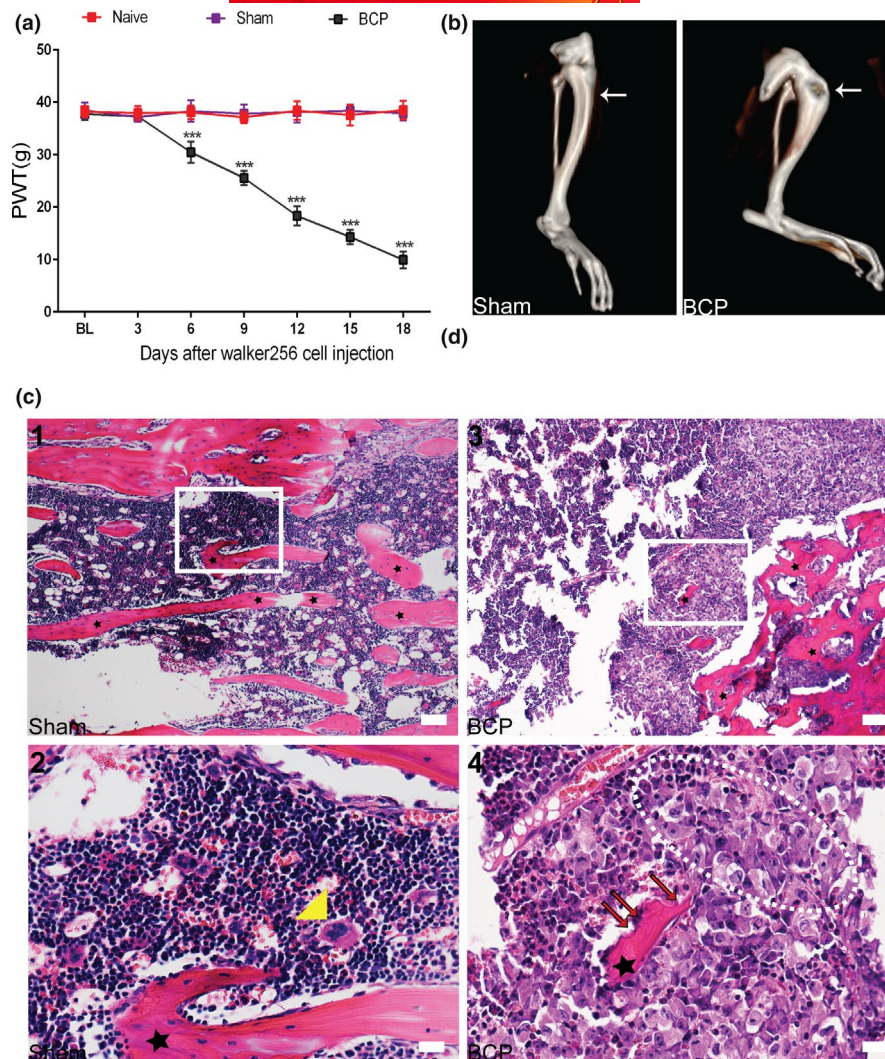


FIGURE 2 A bone cancer pain (BCP) model was successfully established. (a) The mechanical pain threshold of the ipsidal hindfoot in rats with BCP decreased from day 6 to day 18 after surgery (** $p < 0.001$ vs. sham group; $n = 6$, two-way repeated-measures ANOVA). (b) Three-dimensional (3D) CT reconstruction showed significant cortical bone destruction after tumour inoculation. Arrowhead points to the spot where tumour cells caused abnormal bone structure. $n = 10$. (c) (1, 2) Haematoxylin-eosin staining showed that the bone marrow cavity of rats in the sham group was filled with lymphocytes, red blood cells and macrophages (yellow triangle). Regular arrangement of trabecular bone (asterisks) can also be seen in the bone marrow cavity. (3, 4) After tumour inoculation, cancer cells (within the dotted lines) and bone resorption pits (red arrows) appeared in the bone marrow cavity of rats with BCP. Figures c(2, 4) are high-magnification images of the selected area with white frames; $n = 10$. Scale bars: 200 μm (top row), 50 μm (bottom row). BL, baseline. n represents the number of experimental animals in each group

2.7 | siRNA transfection

Nrf2 and HO-1 siRNA duplexes were chemically synthesized by Guangzhou RuiBo Biological Technology Co. According to a previous study (Chen et al., 2019), the sequence of the sense strand of the Nrf2 siRNA was 5'-GAGGAUGGGAAACCUUACUTT-3', and the sequence of the anti-sense strand was 5'-AGUAAGGUUCCCAUCCUCTT-3'. In addition, HO-1 siRNA was designed as described previously (Zhang et al., 2004). The targeted sequence of rat HO-1 siRNA was 5'-CCACACAGCACUACGUAAA-3' (sense) and 5'-UUUACGUAGUGCUGUGUGG-3' (anti-sense). Rats were transfected via an i.t. injection of Nrf2 and HO-1 siRNA (20 nmol, 20 μl) on days 5, 8 and 11 after tumour implantation. To verify the efficiency of inhibiting HO-1 expression, the dorsal horn of the spinal cord segments L3-L5 was obtained 12 days after surgery for real-time quantitative PCR (RT-PCR).

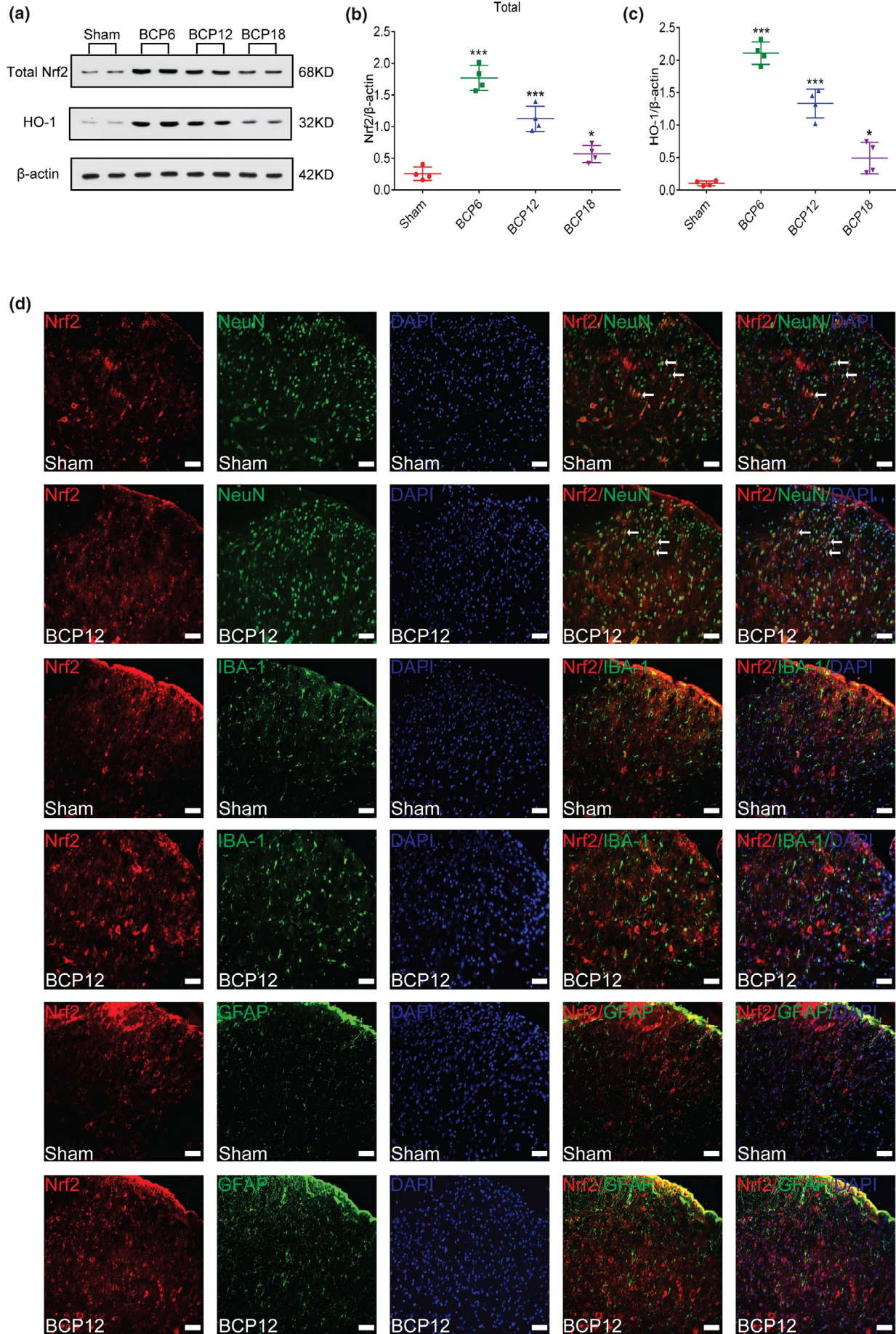
2.8 | Behavioural analysis

In this study, all behavioural tests were performed in a blinded manner in that the tester did not know either the rat's surgical status or the rat's treatment assignment. Mechanical allodynia

was tested by using a set of von Frey monofilaments (BME-404, Institute of Biological Medicine, Academy of Medical Science, China). To detect mechanical sensitivity, the rats were placed in a single, transparent Plexiglas compartment on the metal mesh floor (grid: 0.5 \times 0.5 cm) (10 \times 10 \times 15 cm) and allowed to acclimate for a minimum of 30 min before performing the experiment. The monofilaments were held against the plantar surface of the hind paw until the rats withdrew their paw or licked their feet. The test was repeated three times, with at least 5-min intervals between stimulations (Allette et al., 2014; An et al., 2018). The paw withdrawal threshold (PWT) was expressed as the maximal level tolerance in grams, and the mean PWT of each hind paw was calculated as the average value of the three tests.

2.9 | Histological analysis of bone

To verify the infiltration of cancer cells, 10 rats/group were selected for killing by intraperitoneal injection of excessive sodium pentobarbital (100 mg/kg). The tibia on the surgical side was fixed with 4% paraformaldehyde and decalcified in a 10% ethylenediamine-tetraacetic acid mixture for 24 hr, paraffin-embedded and cut into



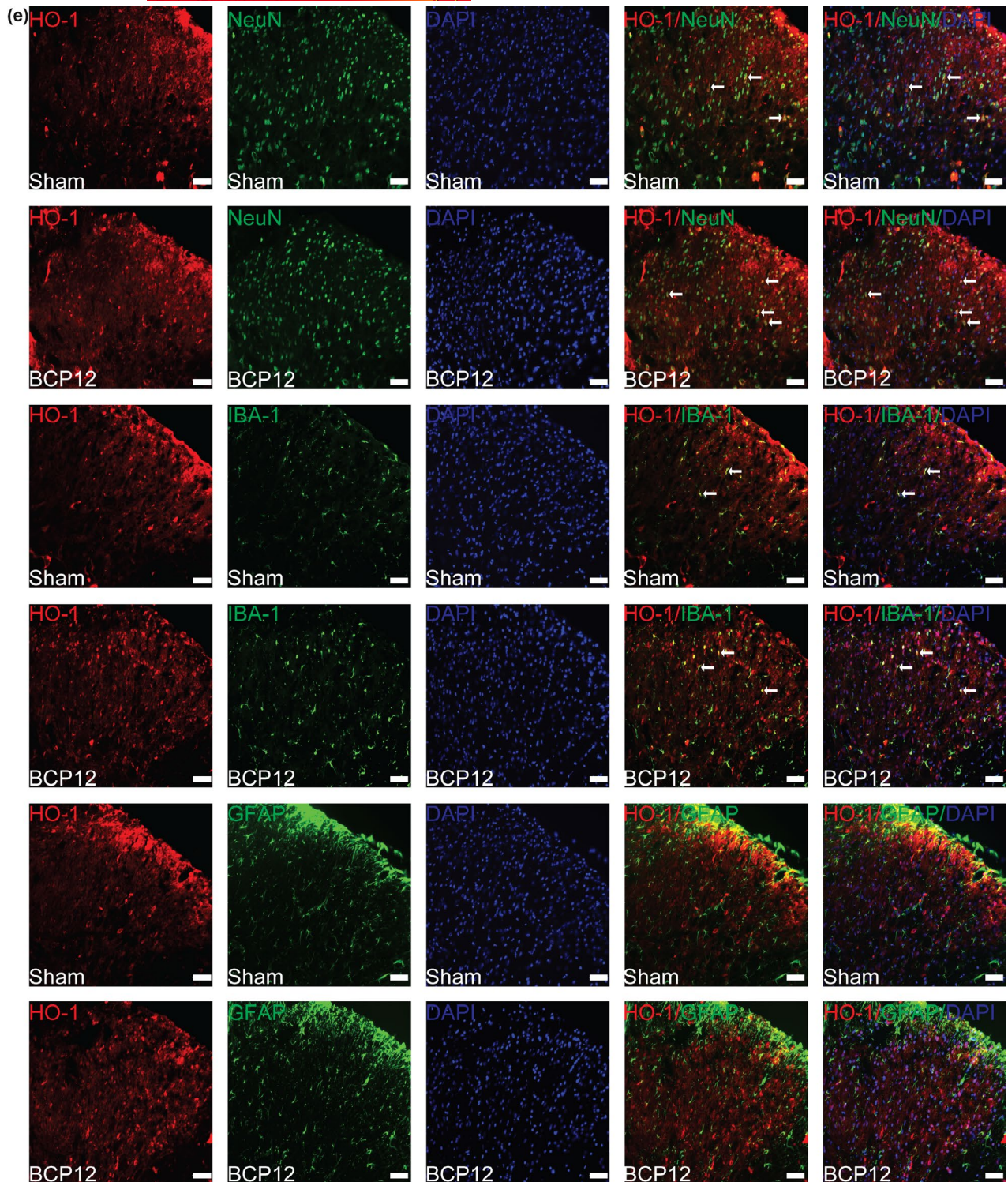


FIGURE 3 Dynamic changes in nuclear factor erythroid 2 (NFE2)-related factor 2 (Nrf2) and heme oxygenase-1 (HO-1) expression and cellular localization after tumour inoculation. (a–c) Western blot analysis showed that after tumour inoculation, Nrf2(a and b) and HO-1(a and c) expression levels in the spinal cord of the model group were significantly increased compared with those in the sham group on days 6, 12 and 18 after the operation ($*p < 0.05$, $***p < 0.001$ vs. sham group; $n = 4$, one-way ANOVA). (d and e) Immunofluorescence results showed that in the dorsal horn of the spinal cord of bone cancer pain (BCP) rats, Nrf2 (red) was primarily expressed in neurons (green) rather than astrocytes (green) or microglia (green), whereas HO-1 (red) was primarily expressed in neurons (green) and partially in microglial cells (green), lacking colocalization with astrocytes (green). Lumbar enlargements were collected on day 12 after the operation or tumour inoculation. Sections were counterstained with DAPI (blue) to label cell nuclei. The white arrows indicate colocalization of Nrf2 and HO-1 with NeuN (neuronal nuclei, neuronal-specific marker), GFAP (glial fibrillary acidic protein, astrocyte specific marker) and Iba-1 (ionized calcium binding adapter molecule 1, microglial-specific marker)-immunoreactive cells in the spinal dorsal horn, respectively; $n = 4$. Scale bar = 50 μm . n represents the number of experimental animals in each group

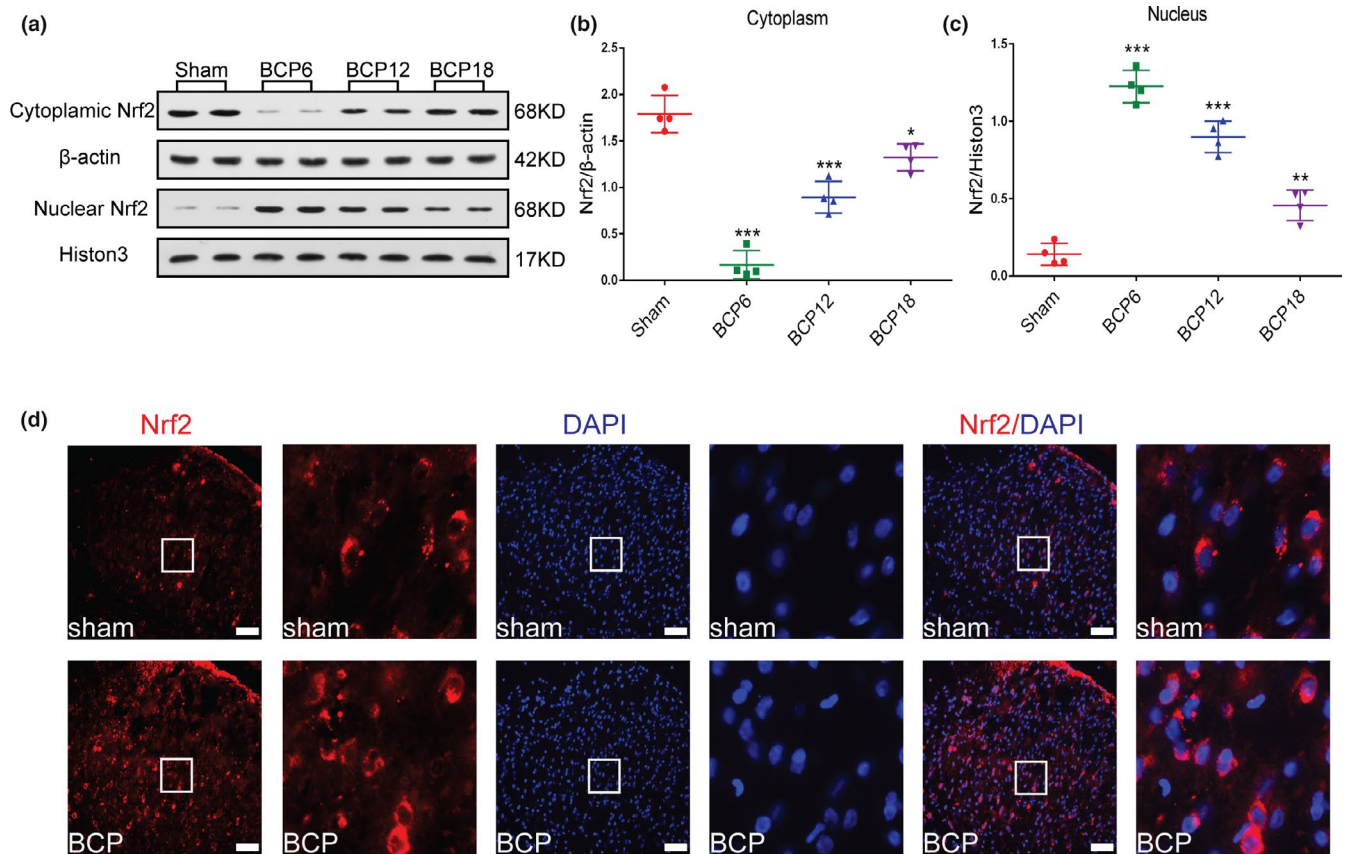


FIGURE 4 Nuclear factor erythroid 2 (NFE2)-related factor 2 (Nrf2) significantly translocates from the cytoplasm to the nucleus after tumour inoculation. (a–c) Western blot analysis revealed dynamic changes in Nrf2 expression in the spinal cord cytoplasm (a and b) and nucleus (a and c) after tumour inoculation ($*p < .05$, $**p < .01$, $***p < .001$ vs. sham group; $n = 4$, one-way ANOVA). (d) Subcellular localization of Nrf2 in the dorsal horn of the spinal cord of rats with bone cancer pain (BCP) (red). DAPI (blue) was used to label the nucleus. High-magnification images of immunofluorescence are indicated in the white box. Lumbar enlargements were collected on day 12 after the operation or tumour inoculation; $n = 4$. Scale bar: 50 μm . n represents the number of experimental animals in each group

8- μm -thick sections. All images were acquired using a 20 \times or 40 \times objective on the microscope (Olympus BX 51)(Xu et al., 2019).

2.10 | Computed tomography reconstruction

To observe the bone destruction, three-dimensional (3D) CT bone reconstruction technology was applied to rats anaesthetized by intraperitoneal injection of sodium pentobarbital (50 mg/kg). Based on our previous study (Xu et al., 2019), CT scan parameters were as follows: helical scanning, 120 kVp, care dose 4D technique, the layer thickness of 1 mm, layer interval of 1 mm, kernel: U30u medium smooth, with CT imaging of SD rat's tibia at high resolution (field of view 100 mm). Finally, Siemens Syngo MMWP post-processing workstation was used to process and analyze the images. Experimental animals were randomized into groups of 10 per group.

2.11 | Western blot

On days 0, 6, 12 and 18 after tumour inoculation, the pain threshold was measured, and four rats/group were deeply anaesthetized by

intraperitoneal injection of sodium pentobarbital (50 mg/kg). RIPA lysis buffer containing a mixture of phosphatase and protease inhibitors was added to the L3–L5 segment of the ipsilateral spinal cord of the rat and ultrasonically lysed into a tissue homogenate. Nuclear protein and cytoplasmic protein were extracted using a nuclear extraction kit and cytosol extraction kit (Beyond Biotechnology), and the supernatant was harvested by centrifugation at 12,000 g for 5 min. The protein concentration was measured using a BCA protein assay (Pierce). An equivalent of 40 μg of protein was separated by 12% SDS-PAGE and transferred to a PVDF membrane. Then, the membrane was blocked with 5% skimmed milk at 20–26°C for 2 hr and probed with Nrf2 (Cat. No:ab92946, abcam 1:1,500), HO-1 (Cat. No:ab13243, abcam 1:1,500), NF- κB p65 (Cat. No:#8242, CST 1:1,000), iNOS (Cat. No:22226-1-AP, proteintech 1:1,000), β -actin (Cat. No:WB0196, Weiao 1:2000), Histone 3 (Cat. No:#4499, CST 1:1,500) and IL-1 β (Cat. No:sc-515598, SAB 1:1,000) overnight at 4°C. Subsequently, the membrane was incubated with horseradish peroxidase-conjugated goat anti-rabbit (Cat. No:115-035-071, Jackson 1:2000) and goat anti-mouse secondary antibodies (Cat. No:115-035-003, Jackson 1:2000) for 2 hr at 20–26°C. Finally, the immunoreactive bands were detected by enhanced chemiluminescence (Thermo Scientific) and X-ray films.

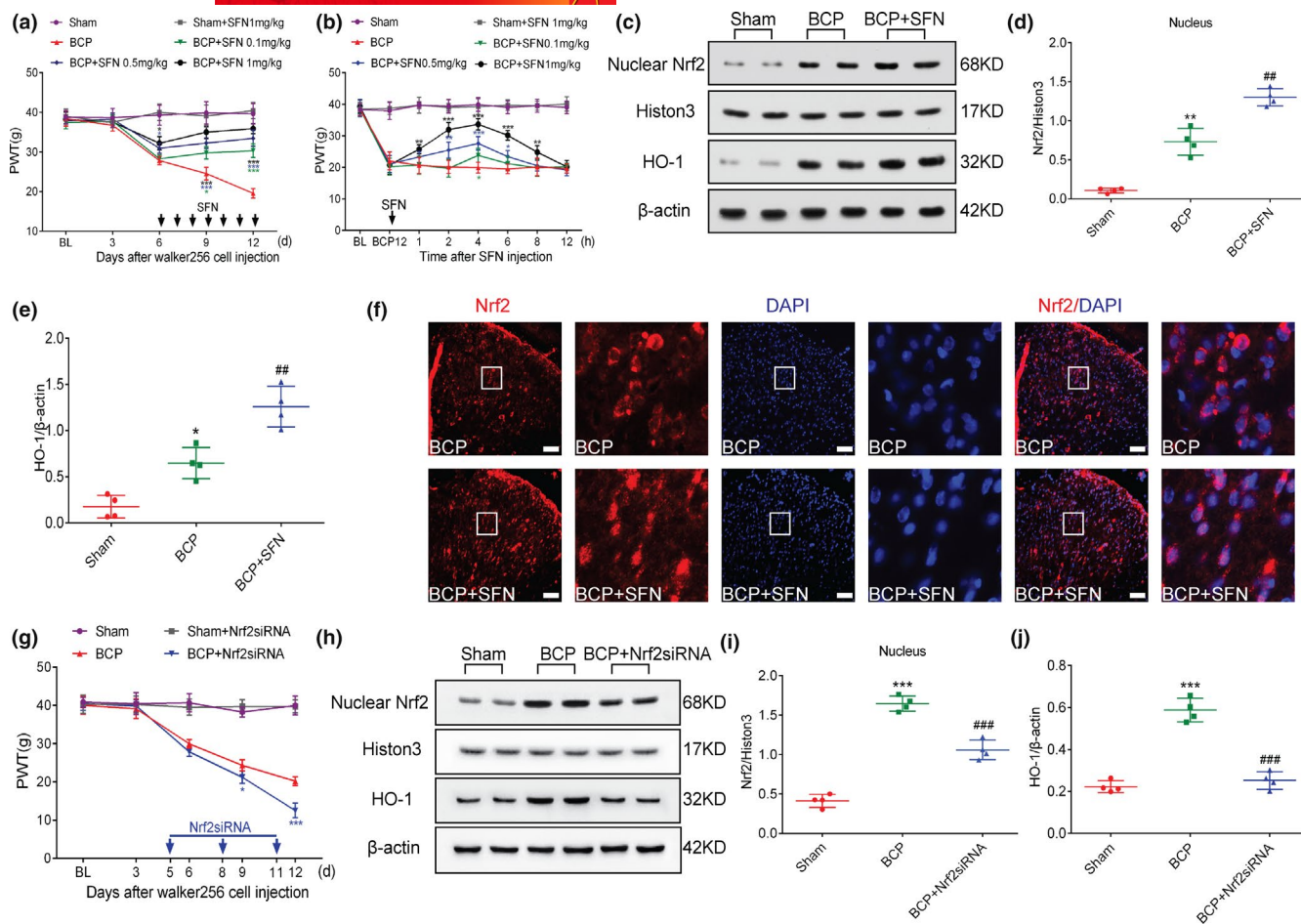


FIGURE 5 Nuclear factor erythroid 2 (NFE2)-related factor 2 (Nrf2) nuclear transcription is associated with the development of pain behaviour in rats with bone cancer pain (BCP). (a, b) Intrathecal administration of sulforaphane (SFN) reduced hyperalgesia in rats with BCP in a dose-dependent manner ($*p < .05$, $***p < .001$ vs. BCP group; $n = 6$, two-way repeated-measures ANOVA). (c–e) Rats were killed on BCP 12 days to collect spinal cord tissue. Western blot analysis showed that SFN further promotes the expression of Nrf2 nucleoprotein (c and d) and its downstream target protein heme oxygenase-1 (HO-1) (c and e) ($*p < .05$, $**p < .01$ vs. sham group; $##p < .01$ vs. BCP group; $n = 4$, one-way ANOVA). (f) Double immunolabelling showed that Nrf2 was almost completely localized in the nucleus after treatment with SFN. High magnification images of immunofluorescence are shown in the white box. Lumbar enlargements were collected on day 12 after tumour inoculation; $n = 4$. Scale bar: 50 μ m. n represents the number of experimental animals in each group. (g) Intrathecal injection of Nrf2 siRNA at 5, 8 and 11 days after the operation significantly induced hyperalgesia in rats with BCP ($*p < .05$, $***p < .001$ vs. BCP group; $n = 6$, two-way repeated-measures ANOVA). (h–k) Rats were killed 12 days after the operation to obtain spinal cord tissue for western blot analysis. Western blot analysis showed that Nrf2 siRNA treatment significantly inhibited BCP-induced Nrf2 nucleoprotein and HO-1 expression ($***p < .001$ vs. sham group; $###p < .001$ vs. BCP group; $n = 4$, one-way ANOVA)

2.12 | Real-time quantitative PCR

On day 12, after tumour inoculation, the pain threshold was measured. Five rats/group were deeply anaesthetized, and the spinal cord L3–L5 segment was taken for lumbar enlargement. Total RNA was extracted using TRIzol reagent (Invitrogen) and then reverse-transcribed the isolated RNA into cDNA. The sample was pre-heated at 95°C for 30 s, followed by 40 amplification cycles (95°C for 5 s and 60°C for 30 s) for cDNA synthesis. The rat primers for HO-1 and β -actin were provided by Sangong Bioengineering Shanghai Co., Ltd. The sequence of the sense strand of the HO-1 was 5'-CAGACAGAGTTTCTTCGCCAGAGG-3', and the sequence of the anti-sense strand was 5'-TGTGAGGACCCATCGCAGGAG-3'. The sequence of the sense strand of the β -actin was

5'-CATCCTGCGTCTGGAACCTGG-3', and the sequence of the anti-sense strand was 5'-TAATGTACGCACGATTTC-3'. The relative gene expression was measured using $2^{-\Delta\Delta Ct}$ method.

2.12.1 | Immunofluorescence

On day 12, after the operation, 4 rats in each group were deeply anaesthetized with sodium pentobarbital (50 mg/kg). The heart was punctured with an intravenous infusion needle towards the ascending aorta, 500 ml thiobarbital sodium [phosphate-buffered saline (PBS)] was injected, and 250 ml of 4% paraformaldehyde was injected. The enlarged lumbar spinal cord was separated from the L3–L5 segment and placed in 4%

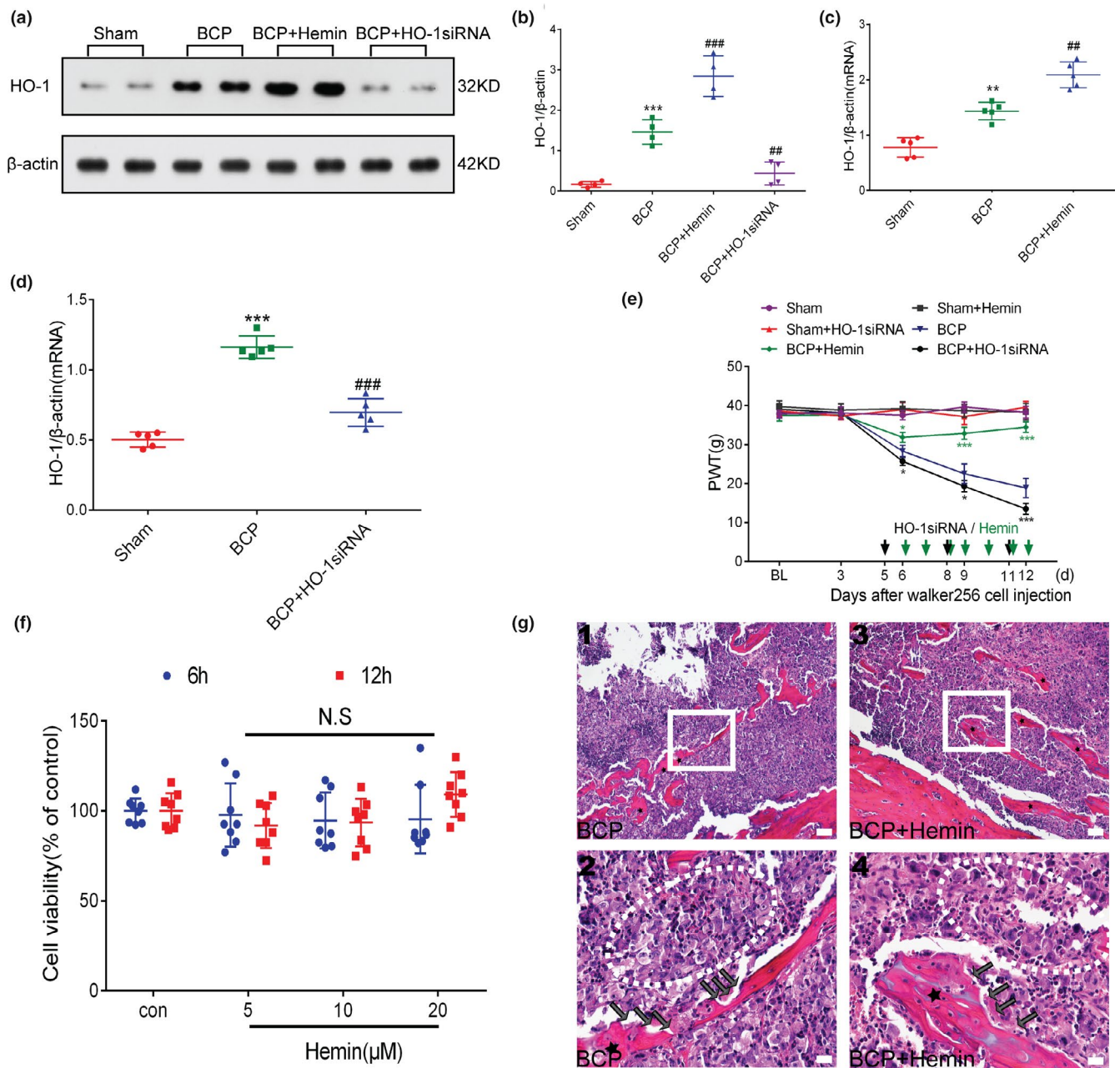


FIGURE 6 Spinal heme oxygenase-1 (HO-1) activation is essential for the regulation of bone cancer pain (BCP). (a–d) After treatment with HO-1 agonist or inhibitor, HO-1 expression in the spinal cord was observed. Rats were killed after 12 days of BCP to collect spinal cord tissue. Hemin and HO-1 siRNA further stimulated and inhibited the expression of HO-1 in the spinal cord of rats with BCP, respectively ($***p < .001$ vs. sham group; $##p < .01$, $###p < .001$ vs. BCP group; $n = 4$, $**p < .01$, $***p < .001$ vs. sham group; $##p < .01$, $###p < .001$ vs. BCP group; $n = 5$, one-way ANOVA). (e) The effects of HO-1 agonist (hemin) and HO-1 inhibitor (HO-1 siRNA) on the paw withdrawal threshold (PWT) in rats with BCP were observed within the indicated duration after inoculation ($*p < .05$, $***p < .001$ vs. BCP group; $n = 6$, two-way repeated-measures ANOVA). (f) Hemin was treated with the indicated concentration for 6 hr and 12 hr. A CCK-8 assay was used to detect Walker 256 cell viability. N.S stands for not statistically significant ($p > .05$ vs. control group, two-way repeated-measures ANOVA). (g) Representative images of haematoxylin-eosin staining showing cancer cell infiltration (cells within the dotted lines) and bone resorption pits (black arrows) on the trabecular surface in the tibial marrow cavity of the BCP (g (1, 2)) and BCP +hemin (g (3, 4)) groups; $n = 10$. Scale bars: 200 μm (top row), 50 μm (bottom row). Rats were killed on BCP 12 days to collect tibia tissues. n represents the number of experimental animals in each group

paraformaldehyde for 6 hr. After dehydration in a gradient sucrose solution (15%–30%) at 4°C for 48 hr, these spinal cord samples were embedded in OCT compound (Sakura) at a temperature of -20°C , cut into 20- μm -thick sections and placed on positively

charged microscope slides. All the frozen sections were washed with PBS and blocked with 5% BSA and 0.2% Triton X-100 at 20–26°C for 1 hr. Then, the slides were incubated with the following primary antibodies at 4°C overnight: Nrf2 (Cat. No:ab89443,

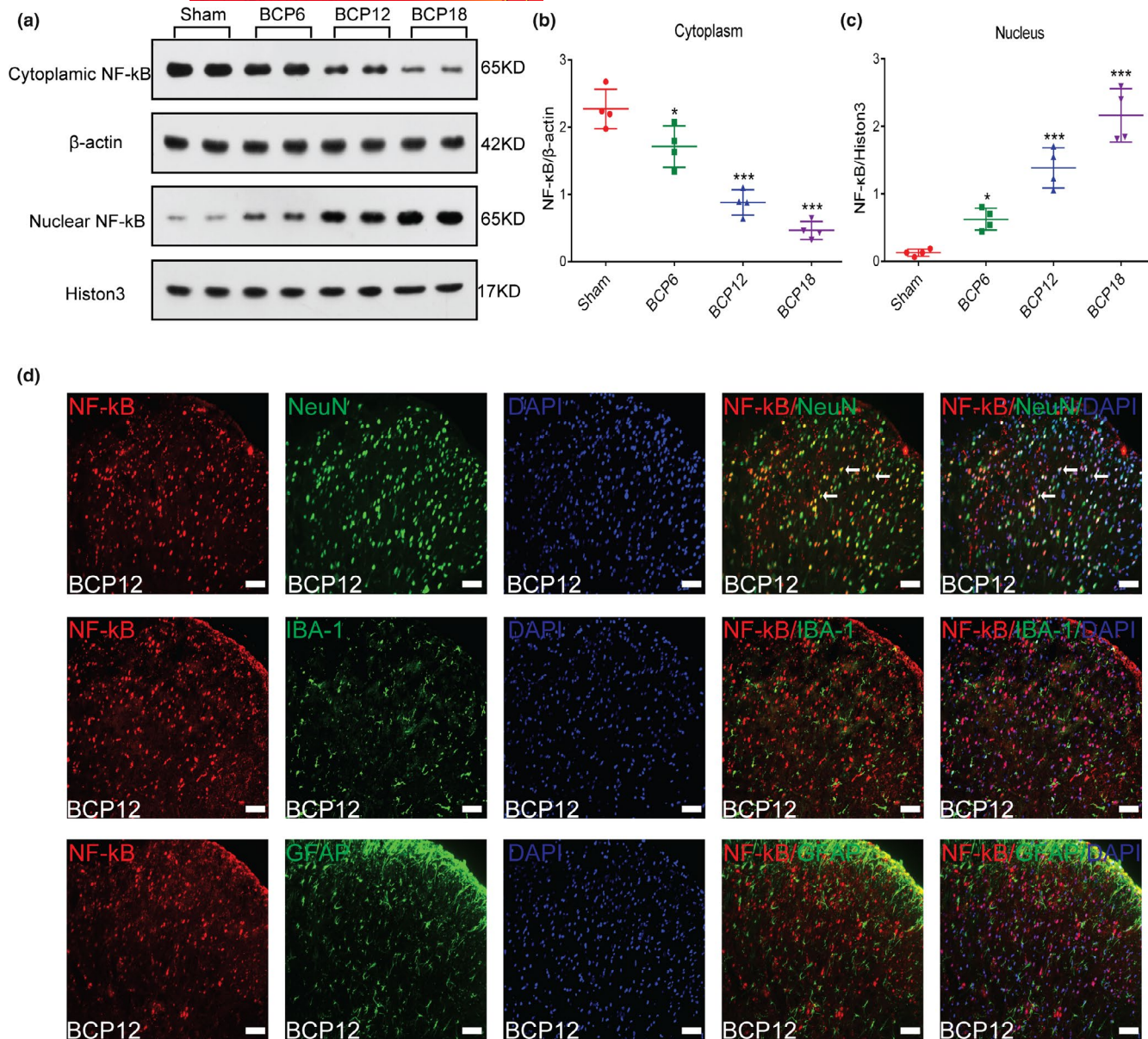


FIGURE 7 Spinal cord nuclear factor-kappa B (NF-κB) translocation from the cytoplasm to the nucleus induced by bone cancer pain (BCP). (a–c) NF-κB cytoplasmic (a and b) and nuclear proteins (a and c) were detected in the spinal cord of rats with BCP by western blot analysis on days 0, 6, 12 and 18 after tumour inoculation ($*p < .05$, $***p < .001$ vs. sham group; $n = 4$, one-way ANOVA). (d) Cellular localization of NF-κB in the spinal dorsal horn of rats with BCP. The immunofluorescence data showed that NF-κB (red) was primarily expressed in neurons (green) rather than astrocytes (green) or microglia (green). Sections were counterstained with DAPI (blue) to label cell nuclei. The white arrows show colocalization of NF-κB with NeuN (neuronal nuclei, neuronal-specific marker), GFAP (glial fibrillary acidic protein, astrocyte specific marker) and Iba-1 (ionized calcium binding adapter molecule 1, microglial specific marker) immunoreactive cells in the spinal dorsal horn. Lumbar enlargements were collected on day 12 after tumour inoculation; $n = 4$. Scale bar: 50 μm . n represents the number of experimental animals in each group

abcam 1:100, mouse source), HO-1 (Cat. No:ab13243, abcam 1:100, rabbit source), NF-κB p65 (Cat. No:AF5006, Affinity 1:100, rabbit source), IBA-1 (Cat. No:ab48004, abcam 1:200, goat source), IBA-1 (Cat. No:#17198, CST 1:100, rabbit source), NeuN (Cat. No:ab279297, abcam 1:100, rabbit source), NeuN (Cat. No:ab104224, abcam 1:100, mouse source), GFAP (Cat. No:#80788, CST 1:100, rabbit source) and GFAP (Cat. No:C9205, Sigma 1:300, mouse source). Subsequently, the sections were incubated for 1 hr at 20–26°C with Alexa Fluor-488

(Cat. No:ab150073, abcam 1:500, donkey anti-rabbit) or Alexa Fluor-488 (Cat. No:ab150105, abcam 1:500, donkey anti-mouse) or Alexa Fluor-488 (Cat. No:ab150129, abcam 1:500, donkey anti-goat) or Alexa Fluor-594 (Cat. No:ab150076, abcam 1:500, donkey anti-rabbit) or Alexa Fluor-594 (Cat. No:ab150108, abcam 1:500, donkey anti-mouse) secondary antibodies. The nuclei were stained with 1 $\mu\text{g}/\text{mL}$ DAPI (H-1200 VECTAS HIELD Antifade Mounting Medium With DAPI). Images were taken using a multiphoton confocal microscope (Leica Microsystems).

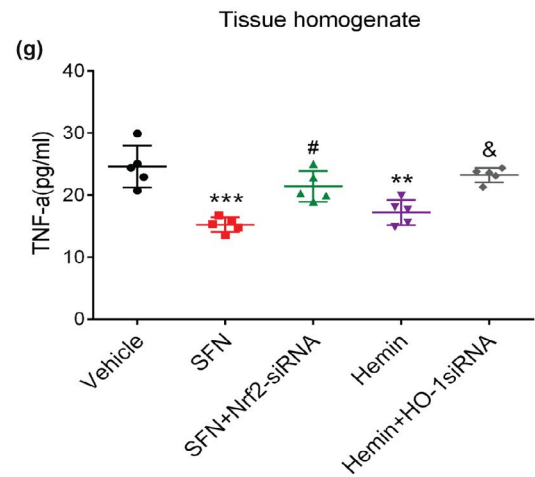
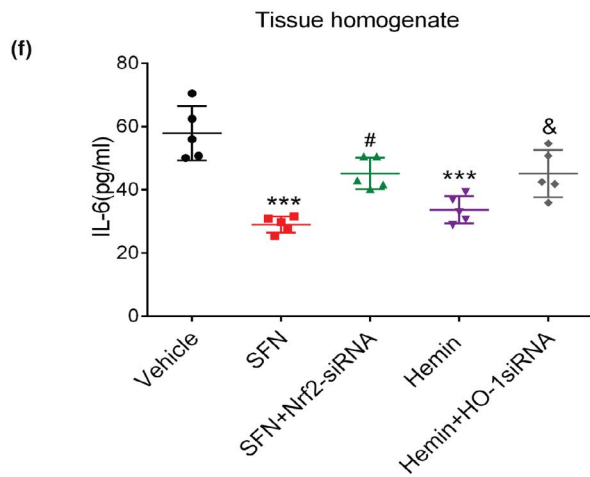
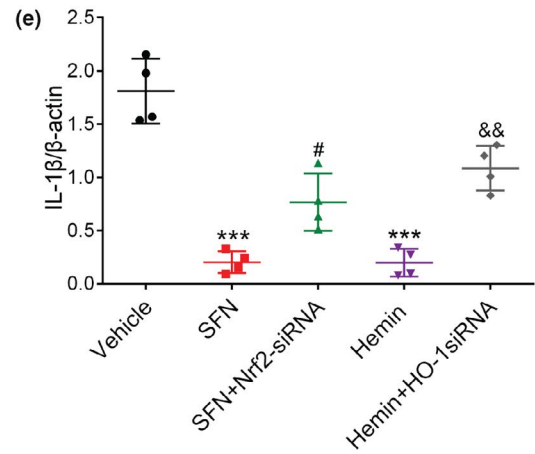
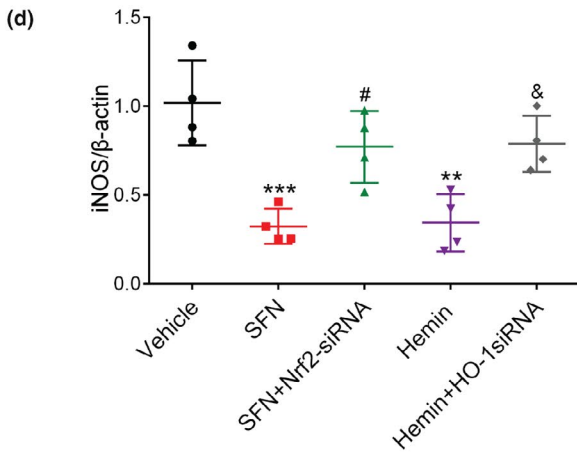
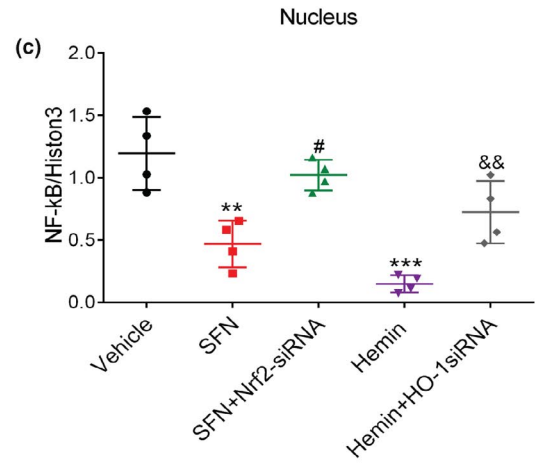
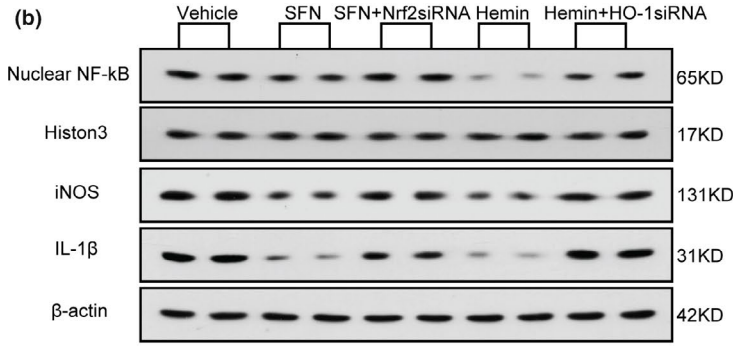
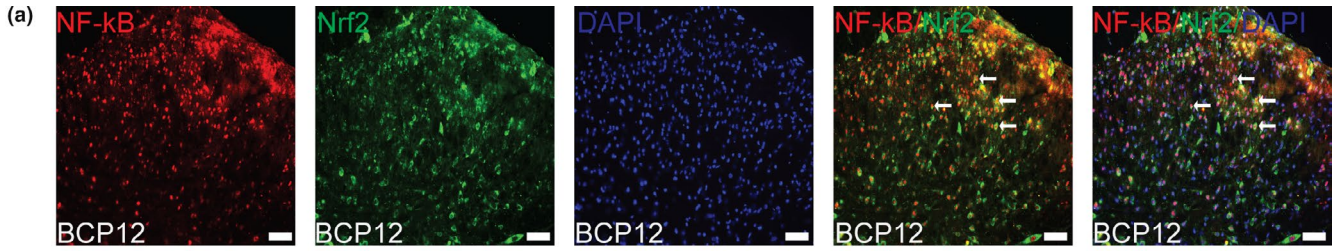


FIGURE 8 The nuclear factor erythroid 2 (NFE2)-related factor 2 (Nrf2)/heme oxygenase-1 (HO-1) axis is involved in the regulation of the nuclear factor-kappa B (NF- κ B) signalling pathway in the spinal cord of rats with bone cancer pain (BCP). (a) NF- κ B (red) and Nrf2 (green) were coexpressed in the dorsal horn of the spinal cord of rats with BCP. Sections were counterstained with DAPI (blue) to label cell nuclei. The white arrows show colocalization of NF- κ B with Nrf2. Lumbar enlargements were collected on day 12 after tumour inoculation; $n = 4$. Scale bar: 50 μ m. (b–g) Treatment with an Nrf2 agonist (sulforaphane, SFN) and HO-1 agonist (hemin) significantly inhibited the activation of NF- κ B and the release of downstream inflammatory factors in the spinal cord of rats induced by BCP. Combined intrathecal administration of siRNA reversed this inhibitory effect. Rats were killed after 12 days of BCP to collect spinal cord tissue. Western blotting was employed to detect the expression of NF- κ B nuclear protein and inflammatory factors (inducible nitric oxide synthase (iNOS) and interleukin-1beta (IL- β)) in the spinal cord of rats with BCP after different treatments (b–e) (** $p < .01$, *** $p < .001$ vs. vehicle treatment group; # $p < .05$ vs. SFN treatment group; &#p < .05, &#p < .01 vs. hemin treatment group; $n = 4$, one-way ANOVA). Enzyme-linked immunosorbent assay (ELISA) was used to detect the expression of inflammatory factors, tumour necrosis factor-alpha (TNF- α) and interleukin-6 (IL-6) (f and g) (** $p < .01$, *** $p < .001$ vs. Vehicle treatment group; # $p < .05$ vs. SFN treatment group; &#p < .05 vs. hemin treatment group; $n = 5$, one-way ANOVA). n represents the number of experimental animals in each group

2.13 | Enzyme-linked immunosorbent assay

According to previous research (Chen et al., 2019), five rats/group were killed 12 days after the operation, and TNF- α and IL-6 cytokines were detected. Under deep anaesthesia, ipsilateral L3–5 spinal cord samples were harvested, dissected on ice, weighed, homogenized in PBS, and the supernatant was collected by centrifugation at 15,000 g at 4°C for 60 min. LinkTech Kit (ELISA) (rat TNF- α (Cat. No:70-EK382/3-96), IL-6 (Cat. No:70-EK306/3-96)) was used to detect the expression of inflammatory molecules.

2.14 | Cell culture

Refer to previous literature (Shenoy et al., 2016), in general, cell lines may be authenticated by short tandem repeat (STR) profiling of the microsatellite regions of DNA (Nims et al., 2010). However, as there is no reference DNA profile of the Walker 256 cell line (Lewis et al., 2013), researchers typically procure cells of a defined passage number from reputable cell banks. To minimize within- and between-laboratory variability in the use of these cells in vivo, it is important that cultured cells are banked and frozen at early passages and that culture conditions including growth media, temperature, humidity and exposure to drugs are standardized (Marx, 2014). In theory, the Walker 256 cell line can be passaged indefinitely. In our study, the walker256 primary cells were a kind gift from Nanjing University of Chinese Medicine and was preserved and frozen during early passage. In the process of subsequent experiments, we provided standardized cell culture conditions. According to previous study (Yu et al., 2020), Walker 256 cells were cultured in RPMI 1640 medium (GIBCO) containing 10% foetal bovine serum (heat-inactivated) (Hyclone), 1% L-glutamine and 2% penicillin/streptomycin (GIBCO) and incubated at 37°C and 5% CO₂. Walker 256 cell line is not listed as a commonly misidentified cell line by the International Cell Line Authentication Committee (ICLAC; <http://iclac.org/databases/cross-contaminations/>).

2.15 | CCK8 assay

Walker 256 cells (1×10^3) were plated into 96-well flat bottom plates in a final volume of 100 μ l/well. Because hemin is not readily soluble

in PBS, it was first dissolved in DMSO (Cat. No:D2650, Sigma-Aldrich) as a 20 mM stock solution and then diluted to the final concentration. Cells were exposed to hemin at concentrations of 0, 5, 10 and 20 μ mol for 6 and 12 hr. At the end of the above-stated exposure periods, CCK-8 (Dojindo) was placed in each of the wells containing the control samples as well as those containing hemin-exposed samples. According to a previous study (Yu et al., 2020), samples were kept in an incubator for 60 min, after which the absorbance was measured using a MultiskanGo Spectrophotometer (United States) at 450 nm optical density. Cell viability (% of control) was determined by the following mathematical relation: [Mean absorbance of exposed/Mean absorbance of control] \times 100].

2.16 | Statistical analysis

All data were collected by researchers who were blinded to the surgeries and reagents used. GraphPad Prism version 6.0 for Windows (RRID:SCR_002798) was used to conduct all statistical analyses. All values were normally distributed by the Shapiro–Wilk test and were reported as mean \pm SD. We did not exclude any animals from data analysis and did not use any test for evaluating outliers of the data (Huang et al., 2019). Nociceptive behavioural tests over time and CCK8 with different doses among groups were tested with two-way, repeated-measures analysis of variance (ANOVA) followed by Bonferroni's post hoc tests (He et al., 2020). Differences in western blot, reverse transcription polymerase chain reaction and enzyme-linked immunosorbent assay values for each group were tested using one-way ANOVA with a Student–Newman–Keuls post hoc test. p values $< .05$ were considered statistically significant.

3 | RESULTS

3.1 | Tumour inoculation induces mechanical allodynia and bone destruction

Von Frey, 3D CT imaging technology and histological analysis were used to confirm the successful preparation of the BCP model. The results showed that compared with the sham group, rats in the



model group exhibited a significant decrease in pain threshold on day 6 after the operation that continued to decrease until the end of the experiment on day 18 after the operation (** $p < 0.001$ vs. sham group; $n = 6$, two-way repeated-measures ANOVA, Figure 2a). The PWT did not show any significant differences between the naive and sham groups ($p > .05$ vs. naive group; $n = 6$, two-way repeated-measures ANOVA, Figure 2a). 3D reconstructed CT images showed significant bone destruction in the tibia of rats with BCP. Conversely, no destructed sign was observed in the bone tissue of rats in the sham group (Figure 2b). The histological analysis showed that naked nuclear lymphocytes, red blood cells and macrophages (yellow triangle) were distributed in the tibial bone marrow cavity of rats in the sham group, and normal trabecular bone structures (asterisks) were visible (Figure 2c(1,2)). After tumour inoculation, there was marked cancer cell infiltration (within the dotted line) and bone resorption pits (red arrow) in the bone marrow cavity of rats with BCP (Figure 2c(3,4)).

3.2 | Spinal expression of Nrf2 and HO-1 is significantly increased after tumour inoculation and is primarily localized in neurons

To study the dynamic expression of Nrf2 and the downstream related protein HO-1 in the spinal cord of rats with BCP, we killed the rats on days 0, 6, 12 and 18 after the operation, and the spinal cord was collected for testing. The results showed that BCP significantly induced the protein levels of total Nrf2 and HO-1 in the spinal cord of rats. With the progression of BCP, the expression of total Nrf2 and HO-1 gradually decreased, but the overall expression was higher than that of the sham group (* $p < 0.05$, ** $p < 0.001$ vs. sham group; $n = 4$, one-way ANOVA, Figure 3a–c).

To examine the cellular localization of Nrf2 and HO-1 in the spinal dorsal horn, we harvested the lumbar spinal tissues from the rats in the sham group and BCP groups on 12 days after the operation. Coimmunostaining images of the spinal dorsal horn in the two groups confirmed that Nrf2 (Figure 3d) signals were colocalized with NeuN-positive (neuronal) cells rather than GFAP-positive (astrocytes) cells or Iba-1-positive (microglial) cells, while HO-1 (Figure 3e) was primarily located in the NeuN-positive cells, with a small proportion is located in the Iba-1-positive cells but no co-localization with GFAP-positive cells.

3.3 | Nrf2 translocates from the cytoplasm to the nucleus after tumour inoculation

Nrf2 is a transcription factor that needs to enter the nucleus to exert its anti-inflammatory and anti-oxidant properties. To study whether Nrf2 nuclear transcription is involved in the development of BCP, we killed rats on days 0, 6, 12 and 18 after surgery to collect spinal lumbar enlargement tissue to detect the expression of Nrf2 protein in

the cytoplasm and nucleus. As shown in Figure 4a–c, on day 6 after the surgery, expression of Nrf2 cytoplasmic protein was significantly decreased, gradually increasing thereafter with the progression of BCP but was lower than that in the sham group (* $p < .05$, ** $p < .001$ vs. sham group; $n = 4$, one-way ANOVA, Figure 4a, b). In contrast, with the progression of BCP, expression of Nrf2 in the nucleus gradually decreased, but overall expression remained higher than that of the sham group. (** $p < .01$, ** $p < .001$ vs. sham group; $n = 4$, one-way ANOVA, Figure 4a, c). These results indicate that BCP induces the transfer of Nrf2 from the cytoplasm to the nucleus.

Next, to further demonstrate that BCP induces the translocation of Nrf2 from the cytoplasm to the nucleus, we killed rats on day 12 of BCP to obtain the spinal cord for immunolabelling of Nrf2 and the nucleus. Immunofluorescence results confirmed that Nrf2 was primarily localized in the cytoplasm of spinal cord dorsal horn neurons in sham rats, whereas in rats with BCP, Nrf2 was localized in the cytoplasm and nucleus. (Figure 4d).

3.4 | Nrf2 nuclear transcription alleviates the mechanical hyperalgesia induced by bone cancer and increases the expression of HO-1

To elucidate whether Nrf2 nuclear transcription is related to the development of behavioural patterns in rats with BCP, rats were treated with SFN for 1 week to promote Nrf2 nuclear transcription after the appearance of symptomatic behaviours of allodynia. Previous *in vitro* experiments demonstrated the anti-cancer properties of SFN. Therefore, to avoid tumour suppression affecting the experimental results, SFN was administered via an intrathecal catheter. Specifically, SFN was administered intrathecally (0.1, 0.5 and 1 mg/kg in a total volume of 20 μ l once a day) for 1 week starting on day 6 after the surgery. As shown in Figure 5a, SFN inhibited bone cancer-induced mechanical hyperalgesia in a dose-dependent manner (* $p < .05$, ** $p < .001$ vs. BCP group; $n = 6$, two-way repeated-measures ANOVA, Figure 5a). To further investigate the analgesic effect of SFN in rats with BCP, single-dose SFN (0.1, 0.5 and 1 mg/kg in a total volume of 20 μ l) was administered intrathecally to rats on day 12 after surgery in this experiment. PWT was measured 1 hr before and 1, 2, 4, 6, 8 and 12 hr after drug administration. Compared with the BCP group, PWT was dramatically augmented from 1 to 8 hr in the 1 mg/kg SFN-treated BCP groups. In the 0.5 mg/kg SFN-treated BCP group, the effects were started at 2 hr after the administration and lasted approximately 4 hr. For the 0.1 mg/kg SFN-treated BCP groups, SFN worked only after 4 hr after injection (* $p < .05$, ** $p < .01$, ** $p < .001$ vs. BCP group; $n = 6$, two-way repeated-measures ANOVA, Figure 5b). However, regardless of repeated or single administration, 1 mg/kg of SFN treatment did not change the PWT of the sham group of rats ($p > .05$ vs. sham group; $n = 6$, two-way repeated-measures ANOVA, Figure 5a, b). In the next molecular experiment, we selected 1 mg/kg as the administration dose. After a week of SFN treatment, the rats were killed on day 12 of BCP for western blot and immunofluorescence. Western blot



results revealed that repeated treatment with 1 mg/kg SFN further increased the expression of nuclear Nrf2 protein (** $p < .01$ vs. sham group; ## $p < .01$ vs. BCP group; $n = 4$, one-way ANOVA, Figure 5c, d) and its downstream target protein HO-1 (* $p < .05$ vs. sham group; ## $p < .01$ vs. BCP group; $n = 4$, one-way ANOVA, Figure 5c,e). The immunofluorescence results showed that Nrf2 in the spinal cord of the BCP group exhibited dual localization in the cytoplasm and nucleus, whereas in the spinal cord of rats with BCP treated with SFN, Nrf2 was localized in the nucleus (Figure 5f).

Next, rats were transfected via an i.t. injection of Nrf2 siRNA (20 nmol, 20 μ l) on days 5, 8 and 11 after tumour implantation to inhibit BCP-induced Nrf2 nuclear transcription. PWT changes were observed in BCP from 6 to 12 days. Similar to SFN treatment, Nrf2 siRNA treatment did not change the PWT of sham group rats ($p > .05$ vs. sham group; $n = 6$, two-way repeated-measures ANOVA, Figure 5g). However, compared with the BCP group, Nrf2 siRNA treatment significantly reduced the PWT in BCP group rats (* $p < .05$, *** $p < .001$ vs. BCP group; $n = 6$, two-way repeated-measures ANOVA, Figure 5g). After Nrf2 siRNA treatment, the rats were killed on day 12 of BCP, and the spinal cord tissue was harvested for western blotting. The results of western blotting showed that Nrf2 siRNA treatment significantly inhibited BCP-induced Nrf2 nucleoprotein and HO-1 expression (*** $p < .001$ vs. sham group; ## $p < .001$ vs. BCP group; $n = 4$, one-way ANOVA, Figure 5h–j).

3.5 | HO-1 is necessary to regulate hyperalgesia in rats with bone cancer pain

Next, to study the effect of HO-1 on rats with BCP, we used hemin and HO-1 siRNA to activate and inhibit the expression of HO-1 in the spinal cord, respectively. Hemin (10 mg/kg, 2 ml, ip) was administered once a day for 1 week starting on day 6 after surgery. Rats were transfected via an i.t. injection of HO-1 siRNA (20 nmol, 20 μ l) on days 5, 8 and 11 after tumour implantation. Spinal cord tissue (L3–L5) samples were acquired from the sham, BCP, hemin and HO-1 siRNA-treated BCP groups on day 12 after the operation. Compared with the BCP group, rats with BCP treated with hemin (BCP+hemin) and HO-1siRNA (BCP+HO-1 siRNA) induced and inhibited HO-1 protein (*** $p < .001$ vs. sham group; ## $p < .01$, ### $p < .001$ vs. BCP group; $n = 4$, one-way ANOVA, Figure 6a, b) and mRNA expression (** $p < .01$, *** $p < .001$ vs. sham group; ## $p < .01$, ### $p < .001$ vs. BCP group; $n = 5$, one-way ANOVA, Figure 6c, d), respectively. In the subsequent experiments, we explored the effect of HO-1 on hyperalgesia in rats with BCP. The withdrawal threshold of rats was measured on days 3, 6, 9 and 12 after surgery. The results showed that hemin increased, whereas HO-1 siRNA reduced, the withdrawal threshold in rats with BCP (* $p < .05$, *** $p < .001$ vs. BCP group; $n = 6$, two-way repeated-measures ANOVA, Figure 6e). However, similar to SFN and Nrf2 siRNA treatment, hemin and HO-1 siRNA treatment did not change the basic pain threshold of the sham groups ($p > .05$

vs. sham group; $n = 6$, two-way repeated-measures ANOVA, Figure 6e).

To investigate whether intraperitoneal administration of hemin has an effect on tumour cell growth, we tested the viability of Walker 256 cells after 6 and 12 hr of hemin treatment. The results showed that hemin did not significantly inhibit Walker 256 cell viability compared with the control group ($p > .05$ vs. control group, two-way repeated-measures ANOVA, Figure 6f). Furthermore, after a week of hemin treatment, we assessed the infiltration of cancer cells in the tibia. Histological analysis showed that in both hemin treatment group and BCP group, the bone marrow cavity of rats with BCP was extensively infiltrated by cancer cells with bone trabecular destruction (Figure 6g). Therefore, intraperitoneal administration of hemin does not affect cancer cell growth.

3.6 | NF- κ B translocates from the cytoplasm to the nucleus in spinal dorsal horn neurons after Walker 256 cell inoculation

Similar to Nrf2, NF- κ B is also a critical transcription factor in cells. Therefore, we explored the nuclear translocation of NF- κ B in the BCP model. Similar to the previous experimental design, we killed rats on days 0, 6, 12 and 18 after surgery to collect enlarged spinal lumbar tissue and observed the changes in NF- κ B cytoplasm and nuclear protein expression. Western blot results demonstrated that compared with the control group, the expression of NF- κ B cytoplasmic protein in the spinal cord of the model group gradually decreased with the progression of BCP (* $p < .05$, *** $p < .001$ vs. sham group; $n = 4$, one-way ANOVA, Figure 7a, b), whereas the nuclear NF- κ B protein expression was increased (* $p < .05$, *** $p < .001$ vs. sham group; $n = 4$, one-way ANOVA, Figure 7a, c).

To further define the cellular localization of NF- κ B in the spinal dorsal horn, triple staining of NF- κ B with three different cell markers (NeuN, GFAP and IBA-1) and DAPI was performed. The results showed that NF- κ B was primarily colocalized with neuronal cells, but not with microglia or astrocytes in rats with BCP (Figure 7d).

3.7 | NF- κ B activation and the associated inflammatory mediator release is regulated by the Nrf2/HO-1 signalling pathway

Some studies have shown that the Nrf2 signalling pathway interacts with the NF- κ B signalling pathway. To determine whether a similar mechanism is involved in this model, we first performed double immunostaining of Nrf2 and NF- κ B in the spinal cord of rats with BCP on day 12. The staining results showed that Nrf2 and NF- κ B were coexpressed in the dorsal horn of the spinal cord in rats with BCP. (Figure 8a).

Next, to explore the specific ways in which the Nrf2 signalling pathway and the NF- κ B signalling pathway interact, we divided the

rats with BCP into five groups: vehicle, SFN treatment, SFN combined with Nrf2 siRNA treatment, hemin treatment and hemin combined with HO-1 siRNA treatment group. SFN (1 mg/kg, 20 μ l) was administered via an intrathecal catheter, and hemin was selected for intraperitoneal injection (10 mg/kg, 2 ml). These drugs were administered once a day for 1 week starting on day 6 after the surgery. Rats were transfected via an i.t. injection of Nrf2 and HO-1 siRNA (20 nmol, 20 μ l) on days 5, 8 and 11 after tumour implantation. On the 12th day after the operation, enlarged rat spinal cord lumbar tissue was collected to observe expression levels of NF- κ B nuclear protein. Compared with the vehicle group, both the SFN treatment and hemin treatment groups significantly inhibited the up-regulation of NF- κ B nuclear protein expression induced by BCP, whereas the combined siRNA treatment reversed this effect (** $p < .01$, *** $p < .001$ vs. vehicle treatment group; # $p < .05$ vs. SFN treatment group; $\&p < .05$, $\&\&p < .01$ vs. hemin treatment group; $n = 4$, one-way ANOVA, Figure 8b, c). Because NF- κ B nuclear translocation leads to the transcriptional activation of inflammatory mediators, such as IL-6, TNF- α , iNOS and IL-1 β . Thus, their expression levels were also determined on day 12 after surgery. The results showed that compared with the vehicle group, SFN and hemin treatments significantly inhibited up-regulation of the TNF- α , IL-1 β , IL-6 and iNOS cytokines induced by BCP. As expected, the blockade of Nrf2 and HO-1 by siRNA partially reversed the SFN- and hemin-induced inhibition of the excessive release of the IL-1 β and iNOS (** $p < .01$, *** $p < .001$ vs. vehicle treatment group; # $p < .05$ vs. SFN treatment group; $\&p < .05$, $\&\&p < .01$ vs. hemin treatment group; $n = 4$, one-way ANOVA, Figure 8b, d–e), IL-6 and TNF- α cytokines (** $p < .01$, *** $p < .001$ vs. vehicle treatment group; # $p < .01$ vs. SFN treatment group; $\&p < .05$ vs. hemin treatment group; $n = 5$, one-way ANOVA, Figure 8f, g).

4 | DISCUSSION

BCP remains a clinical challenge, and the underlying mechanisms are poorly understood. Oxidative stress may be one of the most important mechanisms for the production and maintenance of BCP. In this study, we explored the role of Nrf2 in the development of hyperalgesia and the inflammatory response in a BCP rat model. Importantly, we demonstrated the process of Nrf2 translocation and briefly discussed the putative mechanisms involved in the NF- κ B signalling pathway.

Herein, we demonstrated the following: 1. Expression of Nrf2 and HO-1 in the spinal cord of rats with BCP is significantly increased, and these molecules are primarily localized in the neuronal cells of the spinal dorsal horn. 2. After tumour inoculation, Nrf2 translocates from the cytoplasm to the nucleus. 3. Nrf2 nuclear translocation reduces mechanical hyperalgesia and increases the expression of the downstream-related protein HO-1. 4. HO-1 participates in the regulation of hyperalgesia in rats with BCP. 5. The Nrf2/HO-1 signalling pathway is involved in the regulation of BCP-induced activation of NF- κ B and the release of downstream inflammatory factors. These

findings elucidate the role of Nrf2 in the activation of the NF- κ B signalling pathway and hyperalgesia in rats with BCP.

In this experiment, Walker256 breast cancer cells were implanted into the bone marrow cavity of the rats to establish a sustained and stable pain model. On day 6, after tumour inoculation, rats in the model group showed a significant decrease in the pain threshold that continued to decrease until day 18 after the surgery. The results of haematoxylin–eosin staining and CT showed that the normal trabecular bone structure disappeared, and the bone cortex was destroyed in the model group after tumour inoculation. These results indicate that the BCP model was successfully established.

Accumulating evidence suggested that oxidative stress is a critical contributor to cancer pain, the source of which may be targeted in future pharmacological interventions (Nashed et al., 2014; Ren et al., 2012). Nrf2 is one of the master regulators of endogenous anti-oxidant defence (Schmidlin et al., 2019). In response to oxidative stress, Nrf2 promotes a wide variety of anti-oxidant genes, including HO-1. Therefore, we first studied the expression changes of Nrf2 and HO-1 in the spinal cord of rats with BCP. The results showed that the expression of Nrf2 and HO-1 gradually decreased with the progression of BCP, but the overall expression level was higher than that of the control group. This phenomenon is consistent with the results of neuropathic pain induced by paclitaxel or chronic sciatic nerve injury (Chen et al., 2019; Zhou et al., 2020) but is contrary to the changes in complete Freund's adjuvant (CFA)-induced inflammatory pain (Redondo et al., 2017) and diabetes-induced neuropathic pain (McDonnell et al., 2017). In the latter two models, expression of Nrf2 and HO-1 in the model group was significantly reduced compared with that in the control group. Most findings have shown that the body can initiate defence mechanisms by up-regulating Nrf2 and its target genes when oxidative stress occurs (Loboda et al., 2016; Uddin et al. 2021). However, in the present study, Nrf2 and its downstream target gene expression appeared to increase and then decrease with the progression of bone cancer. We speculate that as bone cancer progresses, excess reactive oxygen species (ROS) can lead to increased oxidation levels and decreased anti-oxidant levels, followed by complete disruption of redox homeostasis. In a previous study (Takizawa et al., 2007), it was found that the activity of several anti-oxidant enzymes in dopaminergic neurons exposed to paraquat was decreased, which may be because of high oxidative levels, resulting in the destruction of several proteins because of oxidation and the inability to function properly. Yuguang Zhao et al. (Tian et al., 2020) also suggested that diabetes-induced oxidative stress can break the feedforward loop connecting Nrf2 and p62 (an autophagy-related protein), which directly leads to decreased anti-oxidant capacity and ROS. This in turn directly decreases anti-oxidant capacity and increases ROS, promoting oxidative damage in the diabetic testis. These data indicate that although bone cancer can lead to an imbalance between the oxidative and anti-oxidant systems, moderate oxidative stress induced by bone cancer increases the expression of Nrf2 during the early stage of BCP (6–12 days of BCP). To some extent, it increases the ability of the body to resist oxidative stress. However, with the continuous progression of bone cancer,



the expression of ROS continues to increase. Excessive oxidative stress leads to the destruction of redox reactions and inhibits the expression of Nrf2. Next, we studied the cellular localization of Nrf2 and HO-1 in the spinal dorsal horn of rats with BCP. In our experiments, Nrf2 was entirely localized in neuronal cells, whereas HO-1 was primarily localized in the neurons in the spinal dorsal horn, with a small proportion was localized in the microglial cells, both lacked colocalization with astrocytes. Interestingly, in the neuropathic pain model caused by paclitaxel (Zhou et al., 2020), both Nrf2 and HO-1 were localized in the neurons, and somewhat in astrocytes and microglia, whereas in the nerve injury-induced neuropathic pain model (Chen et al., 2019), the expression of Nrf2 and HO-1 was detected in the microglial cells. We speculated that this difference in the cell distribution type might represent the different roles of Nrf2 and HO-1 in different pain models.

In response to oxidative stress or exposure to Nrf2 activators, Nrf2 dissociates from Keap1 and translocates into the nucleus, heterodimerizes with small Maf proteins, and transactivates an ARE battery of genes (Tonelli et al., 2018). In a previous chronic pain model, the researchers only focused on the changes in the expression of Nrf2 total protein, ignoring the specific cellular mechanism by which it plays a role in the pain model. Therefore, we studied the subcellular localization of Nrf2 in different physiological states. We found that Nrf2 in the spinal cord of rats in the sham group was primarily located in the cytoplasm and relocated to the nucleus after tumour inoculation. To determine whether the pain behaviour in rats with BCP was related to Nrf2 nuclear transfer, we injected SFN, which chemically modifies the KEAP1 protein to promote Nrf2 nuclear transcription and activates the Nrf2 signalling pathway (Kensler et al., 2013; Zhang & Hannink, 2003). In our *in vitro* study, SFN inhibited the proliferation of Walker 256 breast cancer cells (used in our BCP model) in a dose-dependent manner (supplementary figure(a)). To avoid the confounding contribution of tumour suppression to the analgesic effect of the drug, we used intrathecal administration, which is supposed to only act locally in the spinal cord and DRG (He et al., 2020; Hou et al., 2017). The results showed that intrathecal injection of SFN significantly promoted the nuclear translocation of Nrf2 and HO-1 protein expression in the spinal cord of rats with BCP and reduced the mechanical hyperalgesia of rats with BCP in a dose-dependent manner. Next, to further confirm the role of Nrf2 nuclear transcription in BCP, Nrf2 siRNA was used to inhibit the expression of Nrf2 nuclear protein in the spinal cord of rats with BCP. We found that Nrf2 siRNA significantly inhibited the expression of Nrf2 nucleoprotein and HO-1 protein, inducing mechanical hyperalgesia in rats with BCP. These results revealed that Nrf2 nuclear translocation is involved in BCP. In addition, recent studies have shown that intraperitoneal injection of HO-1 receptor agonists relieves pain to varying degrees (Chen et al., 2015; Liu et al., 2016; Shen et al., 2015). Thus, in the next experiment, we explored the role of HO-1 in mechanical hyperalgesia induced by bone cancer. Hemin and HO-1 siRNA were used to treat rats with BCP. Behavioural results confirmed that activation or inhibition of HO-1 significantly reduces or increases mechanical hyperalgesia, respectively. This indicates that

HO-1 is essential for regulating hyperalgesia in the bone cancer rat model. Interestingly, in the above experiments, we found that agonists (SFN, hemin) and inhibitors (Nrf2 siRNA, HO-1 siRNA) of the Nrf2/HO-1 signalling system did not change the basic pain threshold in the sham group. Therefore, we infer that the Nrf2/HO-1 axis may be necessary to regulate mechanical hyperalgesia in rats with BCP but does not participate in the regulation of pain under normal physiological conditions.

NF- κ B is a redox-sensitive factor that can be activated by ROS and translocate to the nucleus (Bellezza et al., 2012). Herein, we confirmed that with the progression of BCP, the expression of nuclear translocation of NF- κ B in the spinal cord of the model group gradually increased. Our data further show that NF- κ B is primarily expressed in neurons in the dorsal horn of the spinal cord, but not in astrocytes or microglia. However, Zhen-peng Song et al. reported the activation of NF- κ B in astrocytes in the spinal dorsal horn of rats inoculated with walker 256 breast cancer cells (Song et al., 2016), which is not consistent with the previous reports of our laboratory (Wang et al., 2018). This difference may be because of the use of different animal strains, different antibodies or different experimental procedures, which need to be further explored in the future.

The Nrf2 and NF- κ B signalling pathways may interact to control the transcription or function of downstream target proteins. LPS stimulates NF- κ B DNA binding activity, and the levels of the p65 subunit of NF- κ B were significantly higher in the nuclear extracts from the lungs of Nrf2^{-/-} mice than in those from WT mice, suggesting a negative role for Nrf2 in NF- κ B activation (Ahmed et al., 2017). In addition, when prostate cancer cells are briefly exposed to α -tocopheryl succinate, a derivative of vitamin E, Nrf2-dependent downstream HO-1 inhibits the nuclear translocation of NF- κ B (Bellezza et al., 2012). This shows that Nrf2 might negatively regulate the NF- κ B signalling pathway by activating the downstream HO-1. Our immunofluorescence results support this hypothesis; NF- κ B and Nrf2 were entirely coexpressed in the dorsal spinal cord after tumour inoculation. Next, we applied drug intervention to test this hypothesis further. SFN and hemin significantly inhibited BCP-induced NF- κ B activation, and the intrathecal injection of the corresponding siRNA reversed this inhibitory effect. In addition, considering that NF- κ B induces the expression of various inflammatory molecules (IL-1 β , IL-6, TNF- α and iNOS), we examined the expression of related inflammatory molecules. Strikingly, siRNA also reversed the anti-inflammatory effects of SFN and hemin in rats with BCP. These results indicate that the Nrf2/HO-1 signalling axis might be involved in the activation of the BCP-induced NF- κ B signalling pathway.

Increasing evidence shows that the activation of NF- κ B following tissue injury or nerve injury is related to the development and maintenance of neuropathic pain. For example, specific inhibitors or lentiviruses inhibit the activation of NF- κ B at the spinal cord level, which partially prevents the development of neuropathic pain (Ledebner et al., 2005; Meunier et al., 2007). NF- κ B inhibitors can also relieve established neuropathic pain (Lee et al., 2011). In previous studies (Wang et al., 2018), we confirmed that NF- κ B is primarily

located in the spinal dorsal horn neurons of rats with BCP, and intrathecal injection of NF- κ B inhibitors significantly inhibited the expression of proinflammatory molecules and BCP-related behaviours. This phenomenon demonstrates that NF- κ B is involved in the development and maintenance of BCP. Therefore, in this study, we did not prove the role of NF- κ B in BCP.

Notably, our experimental study has some limitations. First, in the current experiment, the cell distribution of Nrf2 and HO-1 was not consistent. In addition to Nrf2, there are also a variety of signalling molecules and transcription factors that are related to the expression of HO-1, such as mitogen-activated protein kinase (MAPK) and activator protein 1 (AP-1) (Singh et al., 2019). Second, we confirmed that in the early stage of BCP (6–12 days of BCP), moderate oxidative stress stimulates the translocation of Nrf2 from the cytoplasm of spinal cord neurons to the nucleus, initiating the body's defence response. Intrathecal injection of SFN for 1 week further promoted the entry of Nrf2 into the nucleus and significantly reduced the hyperalgesia and neuroinflammation induced by bone cancer. However, with the progression of bone cancer, excessive oxidative stress inhibits the expression of Nrf2 in the late stage of BCP (18 days of BCP), which further aggravates the neuroinflammatory response. After 18 days of BCP, whether promoting the entry of Nrf2 into the nucleus reduces the hyperalgesia and neuroinflammation caused by bone cancer needs to be further explored. Finally, in the BCP model, the correlation between the Nrf2 and NF- κ B signalling pathways may not be one-way but, instead, may represent a loop. Several studies have shown that NF- κ B reduces the transcription of ARE genes by increasing the recruitment of histone deacetylase 3 (HDAC3) to the ARE region, thereby inhibiting Nrf2 activation (Ahmed et al., 2017). This phenomenon indicates that NF- κ B negatively regulates the expression of Nrf2, which might explain why Nrf2 and NF- κ B exhibited completely opposite trends with the development of BCP. However, these results need to be further confirmed by subsequent experiments.

In summary, we found that Nrf2 expression in spinal dorsal horn neurons increases after tumour inoculation and translocated from the cytoplasm to the nucleus. The activation of the NF- κ B signalling pathway and the release of downstream inflammatory molecules require regulation by the Nrf2/HO-1 signalling pathway, which might help us understand the reason for an excessive neuroinflammatory response during the development and maintenance of BCP in rats.

ACKNOWLEDGEMENTS

This study was supported by the National Natural Science Foundation of China (81901124, 82001176), Natural Science Foundation of Zhejiang Province of China (LY20H090020, LGF20H090021, LQ19H090007), Medical and Health Science and Technology Research Program of Zhejiang Province (2020RC124, 2020RC122), Science and Technology Project of Jiaxing City (2020AY30009), Key Discipline Established by Zhejiang Province and Jiaxing City Jointly—Pain Medicine(2019-ss-ttyx), Key Discipline of Anesthesiology of Jiaxing City (2019-zc-06) and Jiaxing Key Laboratory of Neurology and Pain Medicine.

All experiments were conducted in compliance with the ARRIVE guidelines.

CONFLICT OF INTEREST

The authors have no potential conflicts of interest to declare.

AUTHOR CONTRIBUTIONS

Jie Fu and Ming Yao designed the study. Chao-bo Ni, Hua-Dong Ni, Huan Pan and Dong-Dong Huang collated the data. Jie Fu and Long-Sheng Xu carried out the data analyses. Yan-bao Sun and Ge Luo produced the initial draft of the manuscript. Jie Fu, Ming-Juan Liu and Ming Yao contributed to drafting the final manuscript. All authors have read and approved the final submitted manuscript.

ETHICAL APPROVAL

All applicable international, national and/or institutional guidelines for the care and use of animals were followed. The experiments presented in this manuscript comply with the current laws of the country in which they were performed.

DATA AVAILABILITY STATEMENT

The data that support the findings of this study are available from the corresponding author upon reasonable request. Some data may not be made available because of privacy or ethical restrictions.

ORCID

Ming Yao  <https://orcid.org/0000-0002-4226-8473>

REFERENCES

- Ahmed, S. M., Luo, L., Namani, A., Wang, X. J., & Tang, X. (2017). Nrf2 signaling pathway: Pivotal roles in inflammation. *Biochimica et Biophysica Acta (BBA) - Molecular Basis of Disease*, 1863, 585–597. <https://doi.org/10.1016/j.bbadis.2016.11.005>
- Allette, Y. M., Due, M. R., Wilson, S. M., Feldman, P., Ripsch, M. S., Khanna, R., & White, F. A. (2014). Identification of a functional interaction of HMGB1 with Receptor for Advanced Glycation End-products in a model of neuropathic pain. *Brain, Behavior, and Immunity*, 42, 169–177. <https://doi.org/10.1016/j.bbi.2014.06.199>
- An, K., Rong, H., Ni, H., Zhu, C., Xu, L., Liu, Q., Chen, Y., Zheng, Y., Huang, B., & Yao, M. (2018). Spinal PKC activation - Induced neuronal HMGB1 translocation contributes to hyperalgesia in a bone cancer pain model in rats. *Experimental Neurology*, 303, 80–94. <https://doi.org/10.1016/j.expneurol.2018.02.003>
- Bellezza, I., Tucci, A., Galli, F., Grottelli, S., Mierla, A. L., Pilolli, F., & Minelli, A. (2012). Inhibition of NF- κ B nuclear translocation via HO-1 activation underlies α -tocopheryl succinate toxicity. *Journal of Nutritional Biochemistry*, 23, 1583–1591. <https://doi.org/10.1016/j.jnutbio.2011.10.012>
- Berti-Mattera, L. N., Larkin, B., Hourmouzis, Z., Kern, T. S., & Siegel, R. E. (2011). NF- κ B subunits are differentially distributed in cells of lumbar dorsal root ganglia in naïve and diabetic rats. *Neuroscience Letters*, 490, 41–45. <https://doi.org/10.1016/j.neulet.2010.12.022>
- Buga, S., & Sarria, J. E. (2012). The management of pain in metastatic bone disease. *Cancer Control*, 19, 154–166. <https://doi.org/10.1177/107327481201900210>
- Chen, H., Xie, K., Chen, Y., Wang, Y., Wang, Y., Lian, N., Zhang, K., & Yu, Y. (2019). Nrf2/HO-1 signaling pathway participated in the protection of hydrogen sulfide on neuropathic pain in rats. *International*



- Immunopharmacology*, 75, 105746. <https://doi.org/10.1016/j.intimp.2019.105746>
- Chen, Y., Chen, H., Xie, K., Liu, L., Li, Y., Yu, Y., & Wang, G. (2015). H2 treatment attenuated pain behavior and cytokine release through the HO-1/CO pathway in a rat model of neuropathic pain. *Inflammation*, 38, 1835–1846. <https://doi.org/10.1007/s10753-015-0161-x>
- Cho, H. Y., Reddy, S. P., & Kleeberger, S. R. (2006). Nrf2 defends the lung from oxidative stress. *Antioxidants & Redox Signaling*, 8, 76–87. <https://doi.org/10.1089/ars.2006.8.76>
- Devesa, I., Ferrández, M. L., Terencio, M. C., Joosten, L. A., van den Berg, W. B., & Alcaraz, M. J. (2005). Influence of heme oxygenase 1 modulation on the progression of murine collagen-induced arthritis. *Arthritis and Rheumatism*, 52, 3230–3238. <https://doi.org/10.1002/art.21356>
- Ferreira-Chamorro, P., Redondo, A., Riego, G., Leáñez, S., & Pol, O. (2018). Sulforaphane inhibited the nociceptive responses, anxiety and depressive-like behaviors associated with neuropathic pain and improved the anti-allodynic effects of morphine in mice. *Frontiers in Pharmacology*, 9, 1332. <https://doi.org/10.3389/fphar.2018.01332>
- Fulas, O. A., Laferriere, A., Stein, R. S., Bohle, D. S., & Coderre, T. J. (2020). Topical combination of meldonium and N-acetyl cysteine relieves allodynia in rat models of CRPS-1 and peripheral neuropathic pain by enhancing NO-mediated tissue oxygenation. *Journal of Neurochemistry*, 152, 570–584. <https://doi.org/10.1111/jnc.14943>
- Guo, G., Peng, Y., Xiong, B., Liu, D., Bu, H., Tian, X., Yang, H., Wu, Z., Cao, F., & Gao, F. (2017). Involvement of chemokine CXCL11 in the development of morphine tolerance in rats with cancer-induced bone pain. *Journal of Neurochemistry*, 141, 553–564. <https://doi.org/10.1111/jnc.13919>
- Hayes, J. D., McMahon, M., Chowdhry, S., & Dinkova-Kostova, A. T. (2010). Cancer chemoprevention mechanisms mediated through the Keap1-Nrf2 pathway. *Antioxidants & Redox Signaling*, 13, 1713–1748. <https://doi.org/10.1089/ars.2010.3221>
- He, X.-T., Hu, X.-F., Zhu, C., Zhou, K.-X., Zhao, W.-J., Zhang, C., Han, X., Wu, C.-L., Wei, Y.-Y., Wang, W., Deng, J.-P., Chen, F.-M., Gu, Z.-X., & Dong, Y.-L. (2020). Suppression of histone deacetylases by SAHA relieves bone cancer pain in rats via inhibiting activation of glial cells in spinal dorsal horn and dorsal root ganglia. *Journal of Neuroinflammation*, 17, 125. <https://doi.org/10.1186/s12974-020-01740-5>
- He, X. T., Zhou, K. X., Zhao, W. J., Zhang, C., Deng, J. P., Chen, F. M., Gu, Z. X., Li, Y. Q., & Dong, Y. L. (2018). Inhibition of histone deacetylases attenuates morphine tolerance and restores MOR expression in the DRG of BCP rats. *Frontiers in Pharmacology*, 9, 509. <https://doi.org/10.3389/fphar.2018.00509>
- Hervera, A., Gou, G., Leáñez, S., & Pol, O. (2013). Effects of treatment with a carbon monoxide-releasing molecule and a heme oxygenase 1 inducer in the antinociceptive effects of morphine in different models of acute and chronic pain in mice. *Psychopharmacology (Berl)*, 228, 463–477. <https://doi.org/10.1007/s00213-013-3053-5>
- Hervera, A., Leáñez, S., Motterlini, R., & Pol, O. (2013). Treatment with carbon monoxide-releasing molecules and an HO-1 inducer enhances the effects and expression of μ -opioid receptors during neuropathic pain. *Anesthesiology*, 118, 1180–1197. <https://doi.org/10.1097/ALN.0b013e318286d085>
- Hervera, A., Leáñez, S., Negrete, R., Motterlini, R., & Pol, O. (2012). Carbon monoxide reduces neuropathic pain and spinal microglial activation by inhibiting nitric oxide synthesis in mice. *PLoS One*, 7, e43693. <https://doi.org/10.1371/journal.pone.0043693>
- Hou, X., Weng, Y., Ouyang, B., Ding, Z., Song, Z., Zou, W., Huang, C., & Guo, Q. (2017). HDAC inhibitor TSA ameliorates mechanical hypersensitivity and potentiates analgesic effect of morphine in a rat model of bone cancer pain by restoring μ -opioid receptor in spinal cord. *Brain Research*, 1669, 97–105. <https://doi.org/10.1016/j.brainres.2017.05.014>
- Hu, X. F., He, X. T., Zhou, K. X., Zhang, C., Zhao, W. J., Zhang, T., Li, J. L., Deng, J. P., & Dong, Y. L. (2017). The analgesic effects of triptolide in the bone cancer pain rats via inhibiting the upregulation of HDACs in spinal glial cells. *Journal of Neuroinflammation*, 14, 213. <https://doi.org/10.1186/s12974-017-0988-1>
- Huang, Y., Chen, S. R., Chen, H., & Pan, H. L. (2019). Endogenous transient receptor potential ankyrin 1 and vanilloid 1 activity potentiates glutamatergic input to spinal lamina I neurons in inflammatory pain. *Journal of Neurochemistry*, 149, 381–398. <https://doi.org/10.1111/jnc.14677>
- Hwang, Y. J., Lee, E. W., Song, J., Kim, H. R., Jun, Y. C., & Hwang, K. A. (2013). MafK positively regulates NF- κ B activity by enhancing CBP-mediated p65 acetylation. *Scientific Reports*, 3, 3242. <https://doi.org/10.1038/srep03242>
- Kane, C. M., Hoskin, P., & Bennett, M. I. (2015). Cancer induced bone pain. *BMJ*, 350, h315. <https://doi.org/10.1136/bmj.h315>
- Kensler, T. W., Egner, P. A., Agyeman, A. S., Visvanathan, K., Groopman, J. D., Chen, J. G., Chen, T. Y., Fahey, J. W., & Talalay, P. (2013). Keap1-nrf2 signaling: A target for cancer prevention by sulforaphane. *Topics in Current Chemistry*, 329, 163–177.
- Ledeboer, A., Gamanos, M., Lai, W., Martin, D., Maier, S. F., Watkins, L. R., & Quan, N. (2005). Involvement of spinal cord nuclear factor kappaB activation in rat models of proinflammatory cytokine-mediated pain facilitation. *European Journal of Neuroscience*, 22, 1977–1986.
- Lee, M. K., Han, S. R., Park, M. K., Kim, M. J., Bae, Y. C., Kim, S. K., Park, J. S., & Ahn, D. K. (2011). Behavioral evidence for the differential regulation of p-p38 MAPK and p-NF- κ B in rats with trigeminal neuropathic pain. *Molecular Pain*, 7, 57. <https://doi.org/10.1186/1744-8069-7-57>
- Lewis, K. M., Harford-Wright, E., Vink, R., & Ghabriel, M. N. (2013). Characterisation of Walker 256 breast carcinoma cells from two tumour cell banks as assessed using two models of secondary brain tumours. *Cancer Cell International*, 13, 5. <https://doi.org/10.1186/1475-2867-13-5>
- Liu, X., Zhang, Z., Cheng, Z., Zhang, J., Xu, S., Liu, H., Jia, H., & Jin, Y. (2016). Spinal heme oxygenase-1 (HO-1) exerts antinociceptive effects against neuropathic pain in a mouse model of L5 spinal nerve ligation. *Pain Medicine*, 17, 220–229.
- Loboda, A., Damulewicz, M., Pyza, E., Jozkowicz, A., & Dulak, J. (2016). Role of Nrf2/HO-1 system in development, oxidative stress response and diseases: An evolutionarily conserved mechanism. *Cellular and Molecular Life Sciences*, 73, 3221–3247. <https://doi.org/10.1007/s00018-016-2223-0>
- Lozano-Ondoua, A. N., Symons-Liguori, A. M., & Vanderah, T. W. (2013). Cancer-induced bone pain: Mechanisms and models. *Neuroscience Letters*, 557, 52–59. <https://doi.org/10.1016/j.neulet.2013.08.003>
- Ma, M., Wang, Z., Wang, J., Wei, S., Cui, J., Wang, Y., Luo, K., Zhao, L., Liu, X., & Wang, R. (2020). Endomorphin analog exhibited superiority in alleviating neuropathic hyperalgesia via weak activation of NMDA receptors. *Journal of Neurochemistry*, 155, 662–678. <https://doi.org/10.1111/jnc.15127>
- Ma, Q. (2013). Role of nrf2 in oxidative stress and toxicity. *Annual Review of Pharmacology and Toxicology*, 53, 401–426. <https://doi.org/10.1146/annurev-pharmtox-011112-140320>
- Mantyh, P. W. (2014). Bone cancer pain: From mechanism to therapy. *Current Opinion in Supportive & Palliative Care*, 8, 83–90. <https://doi.org/10.1097/SPC.0000000000000048>
- Mao-Ying, Q. L., Zhao, J., Dong, Z. Q., Wang, J., Yu, J., Yan, M. F., Zhang, Y. Q., Wu, G. C., & Wang, Y. Q. (2006). A rat model of bone cancer pain induced by intra-tibia inoculation of Walker 256 mammary gland carcinoma cells. *Biochemical and Biophysical Research Communications*, 345, 1292–1298. <https://doi.org/10.1016/j.bbrc.2006.04.186>
- Marx, V. (2014). Cell-line authentication demystified. *Nature Methods*, 11, 483–488. <https://doi.org/10.1038/nmeth.2932>



- McDonnell, C., Leánez, S., & Pol, O. (2017). The induction of the transcription factor Nrf2 enhances the antinociceptive effects of delta-opioid receptors in diabetic mice. *PLoS One*, 12, e0180998. <https://doi.org/10.1371/journal.pone.0180998>
- Meunier, A., Latrémolière, A., Dominguez, E., Mauborgne, A., Philippe, S., Hamon, M., Mallet, J., Benoliel, J. J., & Pohl, M. (2007). Lentiviral-mediated targeted NF- κ B blockade in dorsal spinal cord glia attenuates sciatic nerve injury-induced neuropathic pain in the rat. *Molecular Therapy*, 15, 687–697. <https://doi.org/10.1038/sj.mt.6300107>
- Mohamed, D. M., Shaqura, M., Li, X., Shakibaei, M., Beyer, A., Treskatsch, S., Schäfer, M., & Mousa, S. A. (2020). Aldosterone synthase in peripheral sensory neurons contributes to mechanical hypersensitivity during local inflammation in rats. *Anesthesiology*, 132, 867–880. <https://doi.org/10.1097/ALN.0000000000003127>
- Nashed, M. G., Balenko, M. D., & Singh, G. (2014). Cancer-induced oxidative stress and pain. *Current Pain and Headache Reports*, 18, 384. <https://doi.org/10.1007/s11916-013-0384-1>
- Ni, H., Wang, Y., An, K., Liu, Q., Xu, L., Zhu, C., Deng, H., He, Q., Wang, T., Xu, M., Zheng, Y., Huang, B., Fang, J., & Yao, M. (2019). Crosstalk between NF κ B-dependent astrocytic CXCL1 and neuron CXCR2 plays a role in descending pain facilitation. *Journal of Neuroinflammation*, 16, 1. <https://doi.org/10.1186/s12974-018-1391-2>
- Ni, H., Xu, M., Xie, K., Fei, Y., Deng, H., He, Q., Wang, T., Liu, S., Zhu, J., Xu, L., & Yao, M. (2020). Liquiritin alleviates pain through inhibiting CXCL1/CXCR2 signaling pathway in bone cancer pain rat. *Frontiers in Pharmacology*, 11, 436. <https://doi.org/10.3389/fphar.2020.00436>
- Nims, R. W., Sykes, G., Cottrill, K., Ikononi, P., & Elmore, E. (2010). Short tandem repeat profiling: Part of an overall strategy for reducing the frequency of cell misidentification. *In Vitro Cellular & Developmental Biology. Animal*, 46, 811–819.
- Niu, L., Dai, G. H., He, G. L., Yang, M., Hu, H. M., Liu, Z. K., Qian, N. S., & Chen, Y. L. (2017). Decreased spinal endomorphin-2 contributes to mechanical allodynia in streptozotocin-induced diabetic rats. *Neurochemistry International*, 108, 372–380. <https://doi.org/10.1016/j.neuint.2017.05.014>
- Pauwels, E. K., Erba, P. A., & Kostkiewicz, M. (2007). Antioxidants: A tale of two stories. *Drug News Perspect*, 20, 579–585. <https://doi.org/10.1358/dnp.2007.20.9.1162242>
- Redondo, A., Chamorro, P. A. F., Riego, G., Leánez, S., & Pol, O. (2017). Treatment with sulforaphane produces antinociception and improves morphine effects during inflammatory pain in mice. *The Journal of Pharmacology and Experimental Therapeutics*, 363, 293–302. <https://doi.org/10.1124/jpet.117.244376>
- Ren, B. X., Gu, X. P., Zheng, Y. G., Liu, C. L., Wang, D., Sun, Y. E., & Ma, Z. L. (2012). Intrathecal injection of metabotropic glutamate receptor subtype 3 and 5 agonist/antagonist attenuates bone cancer pain by inhibition of spinal astrocyte activation in a mouse model. *Anesthesiology*, 116, 122–132. <https://doi.org/10.1097/ALN.0b013e31823de68d>
- Schmidlin, C. J., Dodson, M. B., Madhavan, L., & Zhang, D. D. (2019). Redox regulation by NRF2 in aging and disease. *Free Radical Biology & Medicine*, 134, 702–707. <https://doi.org/10.1016/j.freeradbiomed.2019.01.016>
- Shen, Y., Zhang, Z. J., Zhu, M. D., Jiang, B. C., Yang, T., & Gao, Y. J. (2015). Exogenous induction of HO-1 alleviates vincristine-induced neuropathic pain by reducing spinal glial activation in mice. *Neurobiology of Diseases*, 79, 100–110. <https://doi.org/10.1016/j.nbd.2015.04.012>
- Shenoy, P. A., Kuo, A., Vetter, I., & Smith, M. T. (2016). The walker 256 breast cancer cell-induced bone pain model in rats. *Frontiers in Pharmacology*, 7, 286. <https://doi.org/10.3389/fphar.2016.00286>
- Singh, D., Reeta, K. H., Sharma, U., Jagannathan, N. R., Dinda, A. K., & Gupta, Y. K. (2019). Neuro-protective effect of monomethyl fumarate on ischemia reperfusion injury in rats: Role of Nrf2/HO1 pathway in peri-infarct region. *Neurochemistry International*, 126, 96–108. <https://doi.org/10.1016/j.neuint.2019.03.010>
- Song, Z. P., Xiong, B. R., Guan, X. H., Cao, F., Manyande, A., Zhou, Y. Q., Zheng, H., & Tian, Y. K. (2016). Minocycline attenuates bone cancer pain in rats by inhibiting NF- κ B in spinal astrocytes. *Acta Pharmacologica Sinica*, 37, 753–762. <https://doi.org/10.1038/aps.2016.1>
- Suzuki, T., Motohashi, H., & Yamamoto, M. (2013). Toward clinical application of the Keap1-Nrf2 pathway. *Trends in Pharmacological Sciences*, 34, 340–346. <https://doi.org/10.1016/j.tips.2013.04.005>
- Takizawa, M., Komori, K., Tampo, Y., & Yonaha, M. (2007). Paraquat-induced oxidative stress and dysfunction of cellular redox systems including antioxidative defense enzymes glutathione peroxidase and thioredoxin reductase. *Toxicology in Vitro*, 21, 355–363. <https://doi.org/10.1016/j.tiv.2006.09.003>
- Tang, J., Li, Z. H., Ge, S. N., Wang, W., Mei, X. P., Wang, W., Zhang, T., Xu, L. X., & Li, J. L. (2012). The inhibition of spinal astrocytic JAK2-STAT3 pathway activation correlates with the analgesic effects of triptolide in the rat neuropathic pain model. *Evidence-Based Complementary and Alternative Medicine: Ecam*, 2012, 185167. <https://doi.org/10.1155/2012/185167>
- Tebay, L. E., Robertson, H., Durant, S. T., Vitale, S. R., Penning, T. M., Dinkova-Kostova, A. T., & Hayes, J. D. (2015). Mechanisms of activation of the transcription factor Nrf2 by redox stressors, nutrient cues, and energy status and the pathways through which it attenuates degenerative disease. *Free Radical Biology & Medicine*, 88, 108–146. <https://doi.org/10.1016/j.freeradbiomed.2015.06.021>
- Thimmulappa, R. K., Lee, H., Rangasamy, T., Reddy, S. P., Yamamoto, M., Kensler, T. W., & Biswal, S. (2006). Nrf2 is a critical regulator of the innate immune response and survival during experimental sepsis. *Journal of Clinical Investigation*, 116, 984–995. <https://doi.org/10.1172/JCI25790>
- Tian, Y., Song, W., Xu, D., Chen, X., Li, X., & Zhao, Y. (2020). Autophagy induced by ROS aggravates testis oxidative damage in diabetes via breaking the feedforward loop linking p62 and Nrf2. *Oxidative Medicine and Cellular Longevity*, 2020, 7156579. <https://doi.org/10.1155/2020/7156579>
- Tonelli, C., Chio, I. I. C., & Tuveson, D. A. (2018). Transcriptional regulation by Nrf2. *Antioxidants & Redox Signaling*, 29, 1727–1745. <https://doi.org/10.1089/ars.2017.7342>
- Turabi, A., & Plunkett, A. R. (2012). The application of genomic and molecular data in the treatment of chronic cancer pain. *Journal of Surgical Oncology*, 105, 494–501.
- Uddin, M. J., Kim, E. H., Hannan, M. A., & Ha, H. (2021). Pharmacotherapy against oxidative stress in chronic kidney disease: Promising small molecule natural products targeting Nrf2-HO-1 signaling. *Antioxidants (Basel)*, 10.
- Usui, T., Nakazawa, A., Okura, T., Deguchi, Y., Akanuma, S. I., Kubo, Y., & Hosoya, K. I. (2016). Histamine elimination from the cerebrospinal fluid across the blood-cerebrospinal fluid barrier: Involvement of plasma membrane monoamine transporter (PMAT/SLC29A4). *Journal of Neurochemistry*, 139, 408–418. <https://doi.org/10.1111/jnc.13758>
- Villeneuve, N. F., Lau, A., & Zhang, D. D. (2010). Regulation of the Nrf2-Keap1 antioxidant response by the ubiquitin proteasome system: An insight into cullin-ring ubiquitin ligases. *Antioxidants & Redox Signaling*, 13, 1699–1712. <https://doi.org/10.1089/ars.2010.3211>
- von Moos, R., Costa, L., Ripamonti, C. I., Niepel, D., & Santini, D. (2017). Improving quality of life in patients with advanced cancer: Targeting metastatic bone pain. *European Journal of Cancer*, 71, 80–94. <https://doi.org/10.1016/j.ejca.2016.10.021>
- Wang, C., Xu, K. E., Wang, Y. U., Mao, Y., Huang, Y., Liang, Y., Liu, Y., Hao, J., Gu, X., Ma, Z., & Sun, Yu'e (2020). Spinal cannabinoid receptor 2 activation reduces hypersensitivity associated with bone cancer pain and improves the integrity of the blood-spinal cord barrier.

- Regional Anesthesia and Pain Medicine*, 45, 783–791. <https://doi.org/10.1136/rapm-2019-101262>
- Wang, H., Huang, M., Wang, W., Zhang, Y., Ma, X., Luo, L., Xu, X., Xu, L., Shi, H., Xu, Y., Wang, A., & Xu, T. (2021). Microglial TLR4-induced TAK1 phosphorylation and NLRP3 activation mediates neuroinflammation and contributes to chronic morphine-induced antinociceptive tolerance. *Pharmacological Research*, 105482.
- Wang, L.-N., Yao, M., Yang, J.-P., Peng, J., Peng, Y., Li, C.-F., Zhang, Y.-B., Ji, F.-H., Cheng, H., Xu, Q.-N., Wang, X.-Y., & Zuo, J.-L. (2011). Cancer-induced bone pain sequentially activates the ERK/MAPK pathway in different cell types in the rat spinal cord. *Molecular Pain*, 7, 48. <https://doi.org/10.1186/1744-8069-7-48>
- Wang, X. J., Li, Y., Luo, L., Wang, H., Chi, Z., Xin, A., Li, X., Wu, J., & Tang, X. (2014). Oxaliplatin activates the Keap1/Nrf2 antioxidant system conferring protection against the cytotoxicity of anticancer drugs. *Free Radical Biology & Medicine*, 70, 68–77. <https://doi.org/10.1016/j.freeradbiomed.2014.02.010>
- Wang, Y., Ni, H., Li, H., Deng, H., Xu, L. S., Xu, S., Zhen, Y., Shen, H., Pan, H., & Yao, M. (2018). Nuclear factor kappa B regulated monocyte chemoattractant protein-1/chemokine CC motif receptor-2 expressing in spinal cord contributes to the maintenance of cancer-induced bone pain in rats. *Molecular Pain*, 14. <https://doi.org/10.1177/1744806918788681>
- Xu, J., Zhu, M. D., Zhang, X., Tian, H., Zhang, J. H., Wu, X. B., & Gao, Y. J. (2014). NFκB-mediated CXCL1 production in spinal cord astrocytes contributes to the maintenance of bone cancer pain in mice. *Journal of Neuroinflammation*, 11, 38. <https://doi.org/10.1186/1742-2094-11-38>
- Xu, M., Ni, H., Xu, L., Shen, H., Deng, H., Wang, Y., & Yao, M. (2019). B14 ameliorates bone cancer pain through downregulating spinal interleukin-1β via suppressing neuron JAK2/STAT3 pathway. *Molecular Pain*, 15. <https://doi.org/10.1177/1744806919886498>
- Yao, M., Chang, X. Y., Chu, Y. X., Yang, J. P., Wang, L. N., Cao, H. Q., Liu, M. J., & Xu, Q. N. (2011). Antiallodynic effects of propentofylline Elicited by interrupting spinal glial function in a rat model of bone cancer pain. *Journal of Neuroscience Research*, 89, 1877–1886. <https://doi.org/10.1002/jnr.22711>
- Yin, Q., Fan, Q., Zhao, Y. U., Cheng, M.-Y., Liu, H. E., Li, J., Lu, F.-F., Jia, J.-T., Cheng, W., & Yan, C.-D. (2015). Spinal NF-κB and chemokine ligand 5 expression during spinal glial cell activation in a neuropathic pain model. *PLoS One*, 10, e0115120. <https://doi.org/10.1371/journal.pone.0115120>
- Young, I. S., & Woodside, J. V. (2001). Antioxidants in health and disease. *Journal of Clinical Pathology*, 54, 176–186. <https://doi.org/10.1136/jcp.54.3.176>
- Yu, J., Luo, Y., Jin, H., Lv, J., Zhou, T., Yabasin, I. B., & Wen, Q. (2020). Scorpion alleviates bone cancer pain through inhibition of bone destruction and glia activation. *Molecular Pain*, 16. <https://doi.org/10.1177/1744806920909993>
- Zhang, D. D., & Hannink, M. (2003). Distinct cysteine residues in Keap1 are required for Keap1-dependent ubiquitination of Nrf2 and for stabilization of Nrf2 by chemopreventive agents and oxidative stress. *Molecular and Cellular Biology*, 23, 8137–8151. <https://doi.org/10.1128/MCB.23.22.8137-8151.2003>
- Zhang, G., Zha, J., Liu, J., & Di, J. (2019). Minocycline impedes mitochondrial-dependent cell death and stabilizes expression of hypoxia inducible factor-1α in spinal cord injury. *Archives of Medical Science: AMS*, 15, 475–483. <https://doi.org/10.5114/aoms.2018.73520>
- Zhang, X., Shan, P., Jiang, D., Noble, P. W., Abraham, N. G., Kappas, A., & Lee, P. J. (2004). Small interfering RNA targeting heme oxygenase-1 enhances ischemia-reperfusion-induced lung apoptosis. *Journal of Biological Chemistry*, 279, 10677–10684. <https://doi.org/10.1074/jbc.M312941200>
- Zhou, Y. Q., Liu, D. Q., Chen, S. P., Chen, N., Sun, J., Wang, X. M., Cao, F., Tian, Y. K., & Ye, D. W. (2020). Nrf2 activation ameliorates mechanical allodynia in paclitaxel-induced neuropathic pain. *Acta Pharmacologica Sinica*, 41, 1041–1048. <https://doi.org/10.1038/s41401-020-0394-6>
- Zimmermann, M. (1986). Ethical considerations in relation to pain in animal experimentation. *Acta Physiologica Scandinavica. Supplementum*, 554, 221–233.

SUPPORTING INFORMATION

Additional supporting information may be found online in the Supporting Information section.

How to cite this article: Fu, J., Ni, C., Ni, H.-D., Xu, L.-S., He, Q.-L., Pan, H., Huang, D.-D., Sun, Y.-B., Luo, G., Liu, M.-J., & Yao, M. (2021). Spinal Nrf2 translocation may inhibit neuronal NF-κB activation and alleviate allodynia in a rat model of bone cancer pain. *Journal of Neurochemistry*, 158, 1110–1130. <https://doi.org/10.1111/jnc.15468>